

# Optimal Harvest-then-Transmit Scheduling for Throughput Maximization in Time-varying RF Powered Systems (Extended Version)

Feng Shan, *Member, IEEE*, Junzhou Luo, *Senior Member, IEEE*, Qiao Jin, Liwen Cao, Weiwei Wu, *Member, IEEE*, Zhen Ling, *Member, IEEE*, and Fang Dong, *Member, IEEE*,

**Abstract**—Energy harvesting is a promising technique to address the energy hunger problem for thousands of wireless devices. In Radio Frequency (RF) energy harvesting systems, a wireless device first harvests energy and then transmits data with this energy, hence the ‘harvest-then-transmit’ (HTT) principle is widely adopted. We must carefully design the HTT schedule, *i.e.*, schedule the timing between harvesting and transmission, and decide the data transmission power such that the throughput can be maximized with the limited harvested energy. Distinct from existing work, we assume energy harvested from RF sources is time-varying, which is more practical but more difficult to handle. We first discover a surprising result that the optimal transmission power is independent of the transmission time, but solely depends on the RF harvesting power, for a simple case when the energy harvesting is stable. We then obtain an optimal offline HTT-scheduling for the general case that allows the RF harvesting power to vary with time. To the best of our knowledge, it is the first optimal HTT-scheduling algorithm that achieves maximum data throughput for time-varying RF powered systems. Finally, an efficient online heuristic algorithm is designed based on the offline optimality properties. Simulations show that the proposed online algorithm has superior performance, which achieves more than 90% of the offline maximum throughput in most cases.

**Index Terms**—Wireless Communication Networks, Algorithm design, Wireless power transfer, Harvest-then-transmit, Radio frequency energy harvesting, Time-varying wireless power

## I. INTRODUCTION

The energy hunger problem is one of the major issues for thousands of wireless devices nowadays, such as wireless sensors, Internet of Things devices, and autonomous vehicles, affecting their working lifetime and thus user experiences. Energy harvesting is a promising technique being developed to address this problem. New research efforts are continuously being made in this direction to harvest energy from various sources. Some recent research work includes magnetic wireless power transfer [1], [2], harvesting energy from the

Manuscript received Dec. 8, 2023; revised Apr. 29, 2024; accepted May 20, 2024. Date of publication Xxx 00, 2024; date of current version Xxx 00, 2024. This work was supported by the National Key R&D Program of China Grant 2021YFB2900100, National Natural Science Foundation of China Grants 62232004, 62072101, 61972086, the Natural Science Foundation of Jiangsu Province under Grant No. BK20230024, Jiangsu Provincial Key Laboratory of Network and Information Security Grant BM2003201, and Key Laboratory of Computer Network and Information Integration of the Ministry of Education of China Grant 93K-9, partially supported by the Fundamental Research Funds for the Central Universities. (*Corresponding author: Junzhou Luo*)

F. Shan, J. Luo, Q. Jin, L. Cao, W. Wu and Z. Ling are with School of Computer Science and Engineering, Southeast University, Nanjing 211189, Jiangsu, P. R. China (Emails: {shafeng, jluo, jinqiao, caoliwen, weiweiwu, zhenling, fdong}@seu.edu.cn).

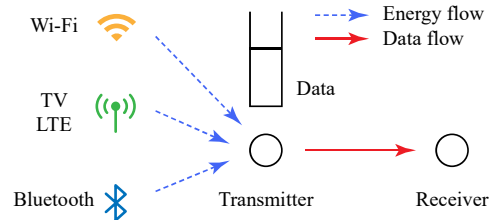


Fig. 1. An illustration of a system that obtains energy from surrounding RF signals and sends its data using the harvested energy.

radio frequency [3], [4], solar energy harvesting for electric autonomous vehicles [5], and underwater ultrasonic wireless power transfer [6].

For the vast majority of wireless devices deployed around the human habitat, energy from radio frequency (RF) is one of the important sources. Since the wireless signal not only carries information but also carries power. Hardware for RF power harvesting has been built to harvest energy from everyday radio frequency signals such as TV broadcast signals [7], WiFi signals [8] and Bluetooth signals [9]. Meanwhile, radio wave interference has been utilized to charge multiple devices concurrently [4]. For a long time, off-the-shelf commercial products on RF wireless power transfer (WPT) have been available from both Powercast [10] and WISP [11]. Fig. 1 illustrates such a system that uses harvested energy to power its operations and transmit data.

A wireless device in an RF powered system usually first harvests energy from RF signals and then transmits data with the harvested energy. There are **three primary reasons** that the two operations execute sequentially. *Firstly*, in low-cost sensors, crucial hardware components like antennas are shared by both the harvesting and transmission modules, preventing simultaneous operations [13], [14]. *Secondly*, most energy harvesting devices, including commercial products from Powercast [10] and WISP [11], use supercapacitors as energy buffers, which inherently cannot support concurrent discharging (transmitting data) and recharging (harvesting energy) [12]. *Lastly*, the limited bandwidth needs to be shared by the two operations. For example, Mohanti *et al.* [8] propose a time-switching strategy that shares the ISM band for WiFi data transmission and RF WPT; more recently, Clerckx *et al.* [28] built a practical energy harvesting system that divides operation time into distinct slots for either receiving power or

transmitting data.

In this paper, we use ‘harvest-then-transmit’ (HTT) to represent the principle of first harvesting energy then transmission data. HTT schedule has already been widely adopted widely [8], [12], [13], [15]–[17], [19], [21], [22].

### A. Related Work

Time-varying is one of the most significant features for general energy harvested from the surrounding environment, including energy harvested from RF signal power sources [13], [15], and from other power sources [18]. Despite tremendous research efforts being spent in this direction, how the time-varying RF power affects the wireless data throughput, even for a simple scenario including only one transmitter and one receiver, is not yet fully investigated.

This paper therefore studies such a fundamental HTT scheduling problem aiming at transmitting the maximum data in a given time duration, assuming the wireless harvesting power is time-varying. More specially, we wish to optimally determine for the transmitter when to do energy harvesting (charging), when to do data transmission (sending), and what transmission power to use, in order to maximize data transmission with the limited and dynamic harvested power.

Some of the most relevant research work includes [12], [15], [19], [20]. Ju *et al.* [19] are among the first group of researchers to investigate this problem, although they assume constant harvesting power. For one transmitter one receiver scenario, they have observed an important tradeoff that setting a longer charging time leads to a shorter sending time but at a higher transmission rate since more energy was charged, while setting a shorter charging duration results in a lower transmission rate but a longer sending duration. They have proposed a way of finding the best time allocation to achieve maximum data throughput. Zhao *et al.* [20] have also studied the same throughput maximization problem and proposed a numerically searching technique to solve it. Zewde *et al.* [15] extends such results on throughput maximization by further considering statistical QoS constraints. Li *et al.* [12] study the network utility (or throughput) maximization problem for cooperative networks. Although Zewde *et al.* [15] and Li *et al.* [12] target advanced topics, they both provide analysis for the simple scenario with only one transmitter and one receiver and constant RF harvesting power. Assuming constant RF harvesting power simplifies the theoretical analysis of HTT and its schedule. However, how the time-varying RF power affects the data throughput remains a theoretically unsolved challenging problem, even for a simple scenario that includes only one transmitter and one receiver.

Distinct from the above most relevant work [12], [15], [19], [20] that aim at the optimal time allocation between charging and sending, we approach the optimal solution from a quite different angle *i.e.*, by targeting the optimal data transmission power. This new approach has led us to discover a surprising result. Our previous work [16], [17] assumes the stable power transfer and studies a different optimization problem, *i.e.*, design an HTT schedule to achieve the minimum delay for transmitting a given set of data packets. These previous works

of ours have inspired the discovery of the basic results of this paper.

Extensive research efforts have been devoted to various topics in RF powered systems. One of the most notable system-building works comes from Clerckx and his coauthors [28], [29]. The system they developed harvests RF energy from the electromagnetic waves of distributed antennas. More specifically, their system has two antennas: one is dedicated to harvesting energy, and the other is for transmitting data. Meanwhile, time is divided into slots, each slot being assigned either for energy harvesting or data transmission. Lopez *et al.* [30] surveyed the research area of RF harvesting, categorizing the harvesting methods based on the number of antennas used and how these antennas are organized to harvest RF energy. Both Lopez *et al.* [31] and Valentini *et al.* [32] allow energy to accumulate over time beyond a single ‘harvest-and-transmit’ round, while the former focuses on a finite battery and finite block length, and the latter studies the problem when the batteries are affected by aging. Huang *et al.* [33] studied a more general problem of one-to-many RF power transfer, investigating how to determine the harvest-transmit time ratio and transmission power. Choi *et al.* [34] allow random access to the wireless broadcast medium. They focus on the harvest-or-access problem for each time slot. Karadag *et al.* [35] explore how to control power and allocate harvest-transmit time, by proving the NP-hardness and then proposing heuristic algorithms.

The time-varying power harvested from harvesting is one of the most important characteristics and is assumed by some recent research work [18]. Qureshi *et al.* [18] design transmission rate selection online algorithm for cognitive radio networks assuming the dynamic power from an energy harvesting source. Kim *et al.* [23] provides a power allocation policy based on reinforcement learning, assuming random energy arrival and time-varying channels. Zhang *et al.* [24] design a general framework to solve the public goods problem for the WPT network, considering the time-varying channel condition.

While general energy harvesting from the surrounding environment has been discussed, RF Wireless Power Transfer (WPT) proves to be a more reliable solution for the vast majority of wireless devices deployed in human habitats.

### B. Motivation and Contributions

From the above discussion, we are motivated by the need to design an efficient *HTT-scheduling* to achieve maximum data throughput for time-varying RF powered systems. The motivations for our work are listed below.

- There is a lack of optimal results for this fundamental problem, despite the tremendous research efforts that have been expended in this direction. Most related work assumes that the wireless power transfer is stable and static. Whether there exists an optimal solution for the fundamental throughput maximization problem for time-varying RF powered systems in a simple scenario with only one transmitter and one receiver is still open.
- We are encouraged by our previous work. Although our previous work [16], [17] studies a different problem and

assumes constant energy harvesting from RF power, we do get inspired by handling the tradeoff of charging and sending. We attack the new optimization problem with a quite different approach, which has led us to discover a surprising result that no existing work has achieved.

In this paper, we attempt to solve the theoretically challenging optimization problem.

- We establish a set of optimality properties for cases with stable energy harvesting, which characterize the necessary conditions for any optimal schedule.
- Our study reveals the surprising discovery that the optimal transmission power is independent of the transmission time but depends solely on the RF harvesting power. This discovery offers valuable insights for addressing related problems in the field.
- Additionally, we introduce an optimal offline HTT-scheduling for the general case that allows RF power to vary with time. To the best of our knowledge, it is the first optimal HTT-scheduling algorithm that achieves maximum data throughput for time-varying RF powered systems.
- We also present the design of an online heuristic algorithm aimed at maximizing throughput in RF power harvesting systems. Its superior performance compared with the optimal offline algorithm is demonstrated by simulations.

The remainder of this paper is organized as follows. In Section II, we formally define the system model and the optimization problem. A set of optimality properties for the *HTT-scheduling* is obtained and presented in Section III. An optimal scheduling algorithm for the defined problem is presented in Section IV and Section V. The online scheduling problem is investigated in Section VI, where an online algorithm is presented. Simulation results are also discussed in the same Section. Section VII concludes this paper.

## II. PROBLEM FORMULATION

### A. System model

We consider a simple communication channel consisting of a data receiver and a wireless-powered data transmitter. The transmitter transmits data to the receiver over an AWGN wireless communication channel, which is widely adopted in the literature [13], [15], [16]. An outside power source, such as TV/WiFi broadcasting signal, cellular signal, or power beacon, is assumed to provide wireless power to the transmitter. Generally, the energy harvested from the outside power source is varying in time. The RF harvesting power is therefore a time-varying function, denoted as  $p(t)$ ,  $0 \leq t \leq T$ , where  $T$  is the length of the duration in consideration.

The transmitter has to first harvest energy before it can transmit data, so the ‘harvest-then-transmit’ principle is used. We therefore define a two-phase cycle that consists of a charging phase and a sending phase. In the charging phase, the transmitter harvests the wireless power, and in the sending phase, it sends data to the receiver. The transmitter repeatedly and continuously switches between the two phases in the time interval  $[0, T]$ . Suppose that there are  $m$  cycles in this interval.

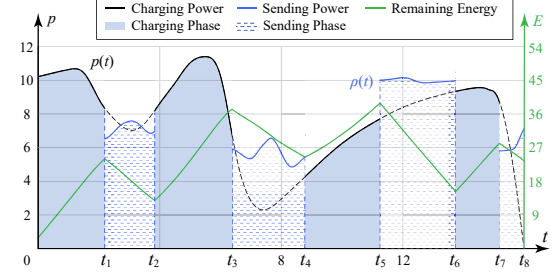


Fig. 2. A wireless transmitter harvests energy in the charging phases and transmits data in the sending phases. The charging power  $p(t)$  is a time-varying function. The phase switching time  $t_i$  and the sending power  $\rho(t)$  are to be determined to maximize throughput. Obviously, the remaining energy increases in the charging phases and decreases in the sending phases.

Thus, there are  $2m$  phases and  $2m$  switches, which occur at time instances  $\{t_1, t_2, \dots, t_{2m}\}$ ,  $0 < t_1 < \dots < t_{2m}$ . The  $2m$  phases are labeled from 1 to  $2m$ , with phase  $i$  starting from time  $t_{i-1}$  and ends at  $t_i$  ( $i = 1, 2, \dots, 2m$ ). The lengths of these phases are to be determined by our algorithm. However, it is assumed that there is a lower bound  $\Delta t$  for the length of any charging phase, which is imposed by the hardware.

Note that we assume  $t_0 = 0$  and the battery has an initial energy  $E_{init}$ . Obviously, phase  $2i-1$  is a charging phase, and phase  $2i$  is a sending phase,  $i = 1, 2, \dots, m$ .

In sending phases, the transmission power is denoted as  $\rho(t)$ , which is subject to the *power constraint* of Eq. (1), where  $\rho_{max}$  is the maximum transmission power imposed by the hardware.

$$0 \leq \rho(t) \leq \rho_{max}, \quad 0 \leq t \leq T. \quad (1)$$

At time  $t$ , the transmitter could choose one of the actions below:

- 1) Consume the energy of the battery at a given power  $\rho(t)$  and transmit data.
- 2) Charge the battery with power  $p(t)$ . The minimum charging phase length is  $\Delta t$ , which is imposed by the hardware.

Fig. 2 illustrates the relations among the notations of the charging phase, the sending phase, the harvesting power (charging power), the transmission power (sending power), and the remaining energy.

### B. Problem formulation

Let  $H(t)$  be the total energy charged into the battery before time  $t$ , which can be calculated as follows.

$$H(t) = \sum_{i=1}^{k-1} \int_{t_{2i-2}}^{t_{2i-1}} p(t) dt + \int_{t_{2k-2}}^{\min\{t, t_{2k-1}\}} p(t) dt,$$

where  $k$  satisfies  $t_{2k-2} < t \leq t_{2k}$ .

Let  $E(t)$  be the total energy consumed before time  $t$ , which can be calculated as follows.

$$E(t) = \sum_{i=1}^{k-1} \int_{t_{2i-1}}^{t_{2i}} \rho(t) dt + \int_{\min\{t, t_{2k-1}\}}^{\min\{t, t_{2k}\}} \rho(t) dt,$$

where  $k$  satisfies  $t_{2k-2} < t \leq t_{2k}$ .

Let  $R(t)$  be the remaining energy in the battery at time  $t$ ,

$$R(t) = E_{init} + H(t) - E(t).$$

We ensure that the remaining energy can not be negative:

$$R(t) \geq 0, \quad \forall t \in [0, T]. \quad (2)$$

Because current technology cannot fully charge the battery wirelessly in a short time, the battery capacity is assumed to be large enough and can never be overcharged. Therefore, the battery capacity does not affect the performance of any schedule.

During the sending phase, the received signal at time  $t$  from the transmitter is given as

$$U_t = h_t X + N_t$$

where  $N_t \sim \mathcal{CN}(0, 1)$  is the circularly-symmetric complex Gaussian noise at the AP with unit variance, and  $h_t$  denotes the channel fading coefficient. Accordingly, the transmission power  $\rho(t)$  at time  $t$  is tightly related to the transmission rate  $r(t)$  through the *power-rate* function of Eq. (3), as commonly assumed [13], [15], [16]

$$r(t) = \log(1 + |h_t|^2 \rho(t)). \quad (3)$$

Note that in some other related works, it is also common to assume  $r(t) = \frac{1}{2} \log(1 + |h_t|^2 \rho(t))$ , and our proposed method is easy to be extended to these cases. In fact, as long as  $r''(t) < 0$ , our main results of this paper hold, more details can be found in the next section. In this paper, we assume  $|h_t| = 1$ . As a consequence, the total amount of data transmitted during the entire time interval  $[0, T]$  can be calculated by the following equation

$$B = \sum_{i=1}^m \int_{t_{2i-1}}^{t_{2i}} \log(1 + \rho(t)) dt. \quad (4)$$

Since we are maximizing the throughput over a fixed period of time, we can simplify the problem by considering the total amount of data transmitted as the throughput. Therefore,  $B$  in Eq. (4) represents the data throughput.

**Definition 1** (The HTT-scheduling problem). *Let  $p(t), t \in [0, T]$  be the harvesting power, the HTT-scheduling problem is to determine the phase switching points  $t_i, i = 1, 2, \dots, 2m$  and the transmission power  $\rho(t)$  in sending phases, so that the data throughput  $B$  in Eq. (4) is maximized while satisfying the power constraint Eq. (1) and remaining energy constraint Eq. (2).*

The HTT-scheduling problem of Definition 1 is called the offline case if the function  $p(t), 0 \leq t \leq T$  is completely known before scheduling. It is called the online problem if  $p(t)$  is not known until time  $t$  reaches the start time of a two-phase cycle.

Unless otherwise specified, we use watt as the unit for power, joule for energy, second for time, and KB for throughput.

### III. THE *wopt* POWER

In this section, we introduce the notion of *wopt* power, which will play a key role in designing an optimal HTT schedule. We use a simplified *HTT-scheduling problem* to explain this notion.

**Definition 2** (Basic HTT-scheduling problem). *An HTT-scheduling problem with the following 2 assumptions is called basic HTT-scheduling problem. 1) The harvesting power  $p(t)$  remains constant for the entire duration of  $[0, T]$ ; and 2) there is no limit on the maximum transmission power  $\rho_{max}$ .*

It is well-known that [12], [15], [19] if the wireless transmitter does not harvest any energy but solely relies on the initial energy  $E_{init}$  for the entire duration of  $T$ , then, because of the concave property of the power-rate function Eq. (3), the optimal transmission power is

$$\rho = \frac{E_{init}}{T}, \quad (5)$$

which depends on both the initial energy and the length of the duration in consideration.

Now we consider the wireless device has another option: It can harvest RF power to charge the battery. In this case, if there are multiple charging phases, we can always move a later charging operation to an earlier time. Therefore, for this case, a single charging phase followed by a single sending phase will produce an optimal solution.

Let us discuss how to determine the switching point between these two phases. Suppose that the phase-switching point is  $t_1$ . Because a single constant transmission power  $\rho$  should be used in the sending phase, we obtain the following equation.

$$E_{init} + pt_1 = \rho(T - t_1).$$

Therefore,

$$t_1 = \frac{\rho T - E_{init}}{\rho + p}. \quad (6)$$

Since the data transmission rate is  $\log(1 + \rho)$  at transmission power  $\rho$ , the total throughput  $B$  can be calculated by  $B = (T - t_1) \log(1 + \rho)$ . Plugging in the expression (6) for  $t_1$ , we obtain the following function (7) for  $B$ . Clearly, it is a function of variable  $\rho$ .

$$B(\rho) = (pT + E_{init}) \frac{\log(1 + \rho)}{\rho + p}. \quad (7)$$

To help understand the function  $B(\rho)$ , we illustrate its shape in Fig. 3(a) when  $p = 10$ ,  $E_{init} = 7.6$  and  $T = 8$ . It can be seen that there is a maximum value of  $B(\rho)$  for  $\rho \in [0, 30]$ . To analytically locate the maximum value of function  $B(\rho)$ , we calculate its first and second order of derivatives as shown below.

$$\begin{aligned} B'(\rho) &= (pT + E_{init}) \left( \frac{\log(1 + \rho)}{\rho + p} \right)' \\ &= \frac{pT + E_{init}}{(p + \rho)^2} \left[ \left( 1 + \frac{p-1}{1+\rho} \right) \frac{1}{\ln 2} - \log(1 + \rho) \right]. \end{aligned}$$

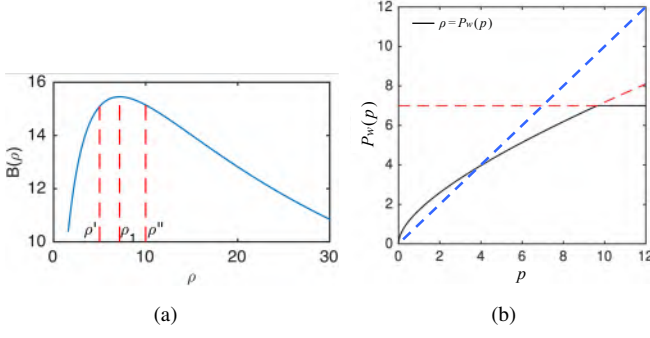


Fig. 3. (a) The shape of  $B(\rho)$  in Eq. (7) when  $p = 10$ ,  $E_{init} = 7.6$  and  $T = 8$ , which is maximized at  $\rho_w \approx 7.2$  and the phase switching time in Eq. (6) is  $t_1 = 2.9$ . (b) The curve of function  $\rho = P_w(p)$  when  $\rho_{max} = 7$ .

Because  $(pT + E_{init})/((p+\rho)^2) > 0$ , we define function  $g(\rho)$  as

$$\begin{aligned} g(\rho) &= B'(\rho)/(pT + E_{init})/(p+\rho)^2 \\ &= (1 + \frac{p-1}{1+\rho}) \frac{1}{\ln 2} - \log(1+\rho). \end{aligned}$$

Obviously, for any given  $\rho$ ,  $g(\rho)$  and  $B'(\rho)$  share the same sign and zero point. Because

$$g'(\rho) = -\frac{p-1}{(1+\rho)^2 \ln 2} - \frac{1}{(1+\rho) \ln 2} = -\frac{p+\rho}{(1+\rho)^2 \ln 2} < 0,$$

$g(\rho)$  monotonically decreases. Hence  $B(\rho)$  is concave and its maximum value can be found at point  $\rho_w$ , such that  $g(\rho_w) = 0$ . By setting  $g(\rho_w) = 0$  we have the following derivations:

$$\begin{aligned} (1 + \frac{p-1}{1+\rho_w}) \frac{1}{\ln 2} &= \log(1 + \rho_w), \\ \text{EXP}(1 + \frac{p-1}{1+\rho_w}) &= 1 + \rho_w, \\ \frac{p-1}{1+\rho_w} \text{EXP}(\frac{p-1}{1+\rho_w}) &= \frac{p-1}{e}, \\ \mathcal{W}(\frac{p-1}{e}) &= \frac{p-1}{1+\rho_w}, \end{aligned}$$

where function  $\mathcal{W}(z)$  is called the Lambert W function [25], which has the following property,

$$\mathcal{W}(z)\text{EXP}(\mathcal{W}(z)) = z.$$

Therefore, we have

$$\rho_w = \frac{p-1}{\mathcal{W}(\frac{p-1}{e})} - 1. \quad (8)$$

Fig. 3(a) shows an example of the function  $B(\rho)$ . Since  $\rho_w \approx 7.2$  for this example,  $t_1 = \frac{\rho_w T - E_{init}}{p+\rho} = \frac{7.2 \times 8 - 7.6}{10 + 7.2} = 2.9$ .

From Eq. (6), we observe that, if  $\rho T \leq E_{init}$ , then  $t_1$  should be 0 or negative, which means no charging is needed. We state the main result in the following lemma, whose correctness follows directly from the above discussion.

**Lemma 1.** If  $E_{init} \leq \rho_w T$ , then the optimal solution for the basic problem in Definition 2 consists of a charging phase and a sending phase. The phase transmission power is  $\rho = \rho_w$  determined by Eq. (8) and switching point is  $t_1$  determined by

Eq. (6). If  $E_{init} \geq \rho_w T$ , then no charging phase is needed, and the transmission power is determined by Eq. (5).

We further have the following important theorem, despite the optimal charging/sending phase switching point, namely  $t_1$  from Eq. (6), depends on  $E_{init}$ ,  $p$  and  $T$ .

**Theorem 1.** The optimal sending power  $\rho_w$  is independent of  $E_{init}$  and  $T$ , and depends only on the harvesting power  $p$  when  $E_{init} \leq \rho_w T$ .

This theorem is quite surprising. It plays a key role in the optimal solutions for the general HTT-scheduling problem defined in Definition 1.

Some previous work in the literature [15], [19] also studied the same basic problem, but they all failed to discover Theorem 1 because they focused on finding the optimal phase length  $t_1$ , while we, instead, focus on computing the optimal transmission power  $\rho$ . In a recent attempt by Zewde *et al.* [15], the optimal harvesting time from Eq. (25) in [15],

$$\tau_B^* = \frac{e^{\mathcal{W}(\frac{p-1}{e})+1} - 1}{p + e^{\mathcal{W}(\frac{p-1}{e})+1} - 1}, \quad (9)$$

is a specially case of our optimal phase switching time  $t_1$  from Eq. (6) by setting  $\rho = \rho_w$ ,

$$t_1 = \frac{\rho_w T - E_{init}}{p + \rho_w} = \frac{(\frac{p-1}{\mathcal{W}(\frac{p-1}{e})} - 1)T - E_{init}}{p + \frac{p-1}{\mathcal{W}(\frac{p-1}{e})} - 1}. \quad (10)$$

Note that  $e^{\mathcal{W}(\frac{p-1}{e})+1} = \frac{p-1}{\mathcal{W}(\frac{p-1}{e})}$  by the definition of the Lambert W function. When  $T = 1$  and  $E_{init} = 0$ , our result Eq. (10) can be reduced to their result Eq. (9). However, we instead, focus on the optimal transmission power, which leads to the surprising new discovery in Theorem 1. Our discovery reveals an essential property of RF powered data transmission that has never been disclosed before.

We now introduce the *wopt* power in preparation for the general case, where the wireless power  $p$  may change from time to time.

**Definition 3** (*wopt* power  $P_w(p)$ ). For any given harvesting power  $p$ , the *wopt* power  $P_w(p)$  is defined as follows.

$$P_w(p) = \min\left\{\frac{p-1}{\mathcal{W}(\frac{p-1}{e})} - 1, \rho_{max}\right\}, \quad (11)$$

where  $\rho_{max}$  is the maximum available transmission power which is imposed by the hardware.

The function  $P_w(p)$  is the most important concept throughout this paper. Fig. 3(b) shows the curve of this function for the range of  $p \in (0, 12)$  and  $\rho_{max} = 7$  to give the reader an intuitive idea of this function. For any given *wopt* power  $\rho$  which is less than  $\rho_{max}$ , we can compute its inverse function to obtain the harvesting power  $p = P_w^{-1}(\rho)$ .

#### IV. AN OPTIMAL OFFLINE SOLUTION FOR DECREASING HARVESTING POWER

In this section and in the following section, we will develop an optimal offline algorithm for the HTT-scheduling problem defined in Definition 1, which is the basis of the algorithm

for the general case investigated in the next section. In this section, we solve a simpler case where the harvesting power function  $p(t)$  is assumed to be monotonically decreasing.

Before we design the algorithm that computes the optimal solution, we first want to see what the optimal solution should be like. We therefore present the following theorems on the optimal solution.

**Theorem 2.** *For HTT-scheduling problem, when the harvesting power  $p(t)$  is monotonically decreasing, there exists an optimal solution in which a power level  $w$  exists such that (1) in any charging phase we have  $p(t) > w$ , (2) in any sending phase we have  $p(t) \leq w, 0 \leq t \leq T$ . The level  $w$  is called the dam height.*

*Proof.* See Appendix A.  $\square$

**Theorem 3.** *In the optimal solution, when the harvest power  $p(t)$  is monotonically decreasing, the sending power of the sending phase should be  $P_w(w)$ , where  $w$  is the dam height.*

*Proof.* See Appendix B.  $\square$

From Theorem 2 and Theorem 3, we have known that there is an important *dam height*, which not only distinguishes charging phases from sending phases but also determines the sending power. Therefore, once the optimal *dam height* is determined, the HTT schedule is determined.

**Definition 4** (Dam  $w$  HTT-schedule). *Given the harvesting power  $p(t)$  and the initial battery energy  $E_{init}$ , the following scheduling is called the Dam  $w$  HTT-schedule.*

- Any charging phase  $[a, b]$  satisfies  $p(t) \geq w, t \in [a, b]$ .
- Any sending phase  $[c, d]$  satisfies  $p(t) \leq w, t \in [c, d]$ , and its sending power is  $P_w(w)$ .

Note that, inside either phase, we may have  $p(t) = w$ . This could occur especially when  $p(t)$  is a constant function.

Now the only question is how to find the optimal *dam height*  $w_{opt}$  such that the Dam  $w_{opt}$  HTT-schedule maximizes data throughput before  $T$ .

We start from the following lemma, which is obviously true with no need of proof.

**Lemma 2.** *In a Dam  $w$  HTT-schedule, when the dam height  $w$  increases, the energy used in sending increases, while charged energy decreases as charging phases shrink, hence the remaining energy  $R(T)$  reduces monotonically.*

Since in the optimal HTT-schedule, there must be no remaining energy in the battery at the ending time  $T$ , our strategy is to search the optimal *dam height*  $w_{opt}$  such that in the Dam  $w_{opt}$  HTT-schedule,  $R(T) = 0$ .

We hence design the *dam raising system* to find the optimal *dam height*. Such a system is built upon the time-power diagram, as presented in Fig. 4. Note that in this diagram, we introduce a virtual phase with a virtual harvesting power  $p(t) = w_{max}$ , where  $w_{max} = P_w^{-1}(\rho_{max})$ ,  $t \in [-E_{init}/w_{max}, 0]$ . This virtual phase is to pre-charge the battery to  $E_{init}$ .

We now introduce the *dam raising system* on the time-power diagram in Fig. 4. The curve of  $p(t)$  is treated as a

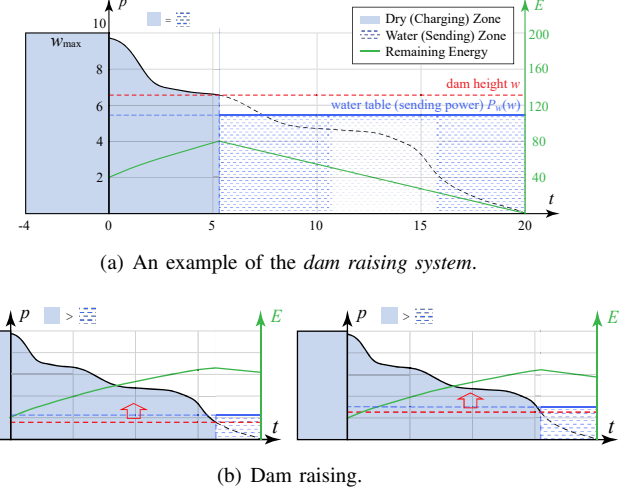


Fig. 4. An example of the *dam raising system* and how the dam is raised. (a) The *dam raising system* is introduced on the time-power diagram, where the curve of  $p(t)$  is treated as a mountain (especially for the general  $p(t)$ ). In this mountain area, a dam is built to hold water. A dam with height  $w$  can hold the water table with height  $P_w(w)$  (see Section III). The dam height  $w$  divides the mountain area into hills and valleys. Only the valley and its underground hold water, no water beneath the surfaces of the hill. The area right beneath the surface of the hill is called the dry zone (charging zone), whose area is actually the amount of energy charged into the battery; the area right beneath the water table is called the water zone (sending zone) whose area is actually the energy consumed for sending data. (b) In the *dam raising system*, the dam height  $w$  is raised slowly to find its optimal position. It starts with  $w = 0$  and stops raising as soon as the dry zone area equals the water zone area. The green curve indicates the remaining energy in the battery, which increases during the charging phase and decreases during the sending phase.

mountain. Although in the current decreasing harvesting power case, there is only one downslope, our system is intended for general  $p(t)$  where both downslopes and upslopes exist, i.e., there are hills and valleys. In this mountain area, we want to build a dam to hold water (in the valley and underground). Assume a dam with height  $w$  can hold the water table with height  $P_w(w)$ . The dam height  $w$  divides the mountain area into hills and valleys. Only the valley and valley underground hold water, no water beneath the surface of the hill. The area right beneath the surface of the hill is called *dry zone*; the area right beneath the water table is called the *water zone*. The dam has the maximum height  $P_w^{-1}(\rho_{max})$  and the water table has the maximum height  $\rho_{max}$ . Hence, the virtual phase is guaranteed to be a charging phase in our system.

Since an area on the time-power diagram represents an amount of energy, the *dry zone* area corresponds to the energy harvested into the battery, while the *water zone* area corresponds to the energy consumed in sending data. Therefore, the difference between the two zone areas is the remaining energy  $R(T)$ . In Fig. 4, the green curve with its corresponding right y-axis indicates the remaining energy in the battery, which increases during the charging phase and decreases during the sending phase.

The core of the *dam raising system* is to raise the dam height from  $w = 0$ , and stop as soon as the dry zone area equals the water zone area. Then the optimal dam height and the optimal water table are found. At the very beginning, the entire area

is a dry zone with no water zone. As the dam height is raised, the dry zone shrinks horizontally, while the water zone grows both horizontally and vertically. Hence, a unique dam height can be found that equals the two zone areas. The dam raising stops at this height.

For any *Dam w HTT-schedule*, it is easy to compute the remaining energy  $R(t)$  at any time  $t \in [0, T]$ . And  $R(t)$  is illustrated by the green remaining energy curve on the diagram in Fig. 4. Let a procedure `is_shortage( $t_s, t_e, E_0, w$ )` checks whether any part of the remaining energy curve in duration  $[t_s, t_e]$  goes below 0 which means energy shortage and infeasible schedule, where  $E_0$  is the initial energy for  $[t_s, t_e]$ , and  $w$  is the dam height. The procedure returns *true* if there is any shortage, *false* if the schedule is feasible. Obviously, the time complexity of this check is  $O(|t_e - t_s|)$ . Hence, we want to find the highest dam height  $w$  such that `is_shortage(0, T,  $E_{init}$ ,  $w$ )` returns *false*.

In the formal algorithm, the process of dam raising can be efficiently speeded up by bisection searching. Algorithm `dam_raising_shotg` provides formal details.

A simple call to `dam_raising_shotg(0, T,  $E_{init}$ )` will return the optimal dam height.

**Theorem 4.** *Algorithm `dam_raising_shotg(0, T,  $E_{init}$ )` computes the optimal HTT schedule, and time complexity of the algorithm is  $O(T \cdot \log(\frac{\rho_{max}}{\Delta}))$ , where  $\Delta$  is the desired accuracy.*

*Proof.* See Appendix C. □

## V. THE OPTIMAL OFFLINE SOLUTION FOR GENERAL HARVESTING POWER

The section focuses on the general harvesting power case and extends results for the special case of the monotonically decreasing harvesting power. Before we design the algorithm that computes the optimal solution, we first present the following theorems on the optimal solution. It is not hard to see that the following theorems are similar to those in the previous section.

**Theorem 5.** *For the general HTT-scheduling problem, when the harvesting power  $p(t)$  is a general function, in the optimal schedule, there exists a set of time  $\tau_i$ , and the power level  $w_i$  for interval  $[\tau_{i-1}, \tau_i]$ , in which (1) for any charging phase, we*

---

### Algorithm 1: `dam_raising_shotg( $t_s, t_e, E_0$ )`

---

```

1  $w_{lower} = 0;$ 
2  $w_{upper} = \rho_{max};$ 
3 while  $w_{upper} - w_{lower} > \Delta$  do
4    $w = \frac{w_{upper} + w_{lower}}{2};$ 
5   if is_shortage(0, T,  $E_{init}$ ,  $w$ )=false then
6      $w_{lower} = w$ 
7   else
8      $w_{upper} = w$ 
9   end
10 end
11 return  $w$ 

```

---

have  $p(t) > w_i$ , (2) for any sending phase, we have  $p(t) \leq w_i, 0 \leq t \leq T, i = 1, 2, \dots, n$ , unless  $p(t)$  monotonically increases in  $[\tau_{i-1}, \tau_i]$ . The power level  $w_i$  is called the dam heights.

*Proof.* See Appendix D. □

**Lemma 3** (Expanding and shrinking). *Suppose  $w$  and  $\rho$  are the dam height and sending power in a sending phase. If  $P_w(w) < \rho$  ( $P_w(w) > \rho$ ) satisfies, then there exists an operation that expands (shrinks) a sending phase via including (excluding) a small duration at both ends while meeting the following constraints.*

- The operation doesn't change the energy consumption.
- The operation doesn't decrease the throughput.

*Proof.* See Appendix E. □

**Theorem 6.** *In any sending phase of the optimal HTT schedule, the sending power is  $P_w(w)$ , where  $w$  is the dam height of the sending phase.*

*Proof.* See Appendix F. □

Due to the similarity between these theorems and the theorems in the previous section, *dam raising system* can be conveniently extended to the general  $p(t)$  function. Recall that the dam height is raised slowly (so as the water table), and the dam height stops rising once the dry zone area equals the water zone area, which indicates the harvesting energy is used up in sending data. The dam height and water table are raised exactly the same way for the general  $p(t)$  function. One of the differences is that there may be more than one dry zone and more than one water zone. The dam height will meet each valley in order when it rises. When the dam height is raised, the total dry zone area grows, but the total water zone area shrinks, e.g., Lemma 2 still holds. We stop when the two areas are equal. We define such a revised algorithm `dam_raising_general`. This algorithm is executed on the part of the  $p(t)$  from Fig. 2, and the results are given in Fig. 5.

However, the biggest difference for the general  $p(t)$  function is that it is not always possible that one dam height can make the dry zone area be equal to the water zone area. If we consider a longer  $p(t)$  function from Fig. 2, then the problem arises. As in Fig. 6(a), since the dry zone in  $[t_4, t_a]$  is larger than the following water zone, the total area of the dry zone is larger than that of the water zone. We may want to raise the dam to enlarge the charging zone and shrink the sending zone. However, the raise is impossible, because we already have the two zones equal before time  $t_4$ , i.e., the green remaining energy curve touches the x-axis at time  $t_4$ . Note that although  $R(t_4) = 0$ , there is still a certain amount of energy at time  $t_4$  to keep the device functional which is not considered in the *dam raising system* design. So there is no single dam height for the entire duration  $[0, T]$  such that the two zones before  $T$  are equal.

In conclusion, throughout the entire duration  $[0, T]$ , the optimal dam height does not necessarily stay unchanged. Instead, it may change multiple times. Assume it changes at time  $t = \tau_i, i = 1, 2, \dots, n$ , and stays constant in all adjacent

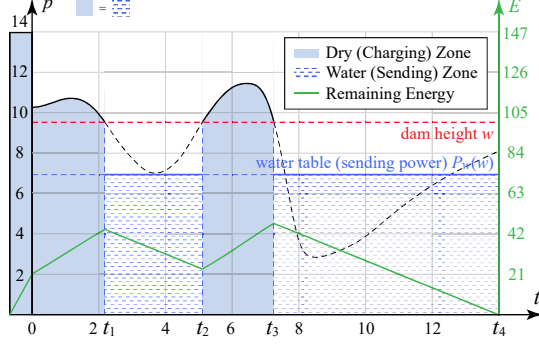
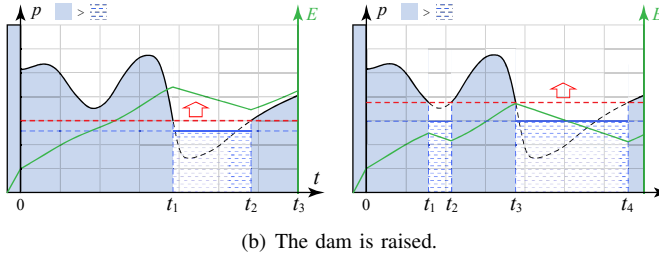
(a) The *dam raising system* for general harvesting power.

Fig. 5. The dam is raised in the *dam raising system* for general harvesting power. (a) For general  $p(t)$ , there are more than one dry zone and water zones. However, all underground water is connected, so they share the same water table in all valleys. (b) When the dam is raised, the water table rises too. The dam raising will create new valleys and open new water zones. As the dam height  $w$  grows larger, the green remaining energy curve increases less but decreases in a larger slope, as a result, this curve generally becomes lower in position. We stop raising once the green curve touches the x-axis because that means the battery is energy-critical at the touch point.

cycles in  $[\tau_{i-1}, \tau_i]$  at  $w_i$ . Now, the problem becomes how to find all the dam height  $w_i$  and the dam height changing points  $\tau_i, i = 1, 2, \dots, n$ .

Before we go any further with the algorithm, we first investigate some optimality properties of the optimal dam height.

**Lemma 4.** *Any two distinct dam heights from two disjoint durations can be equalized to transmit more data in these two durations, unless infeasible solution results.*

*Proof.* See Appendix G.  $\square$

**Lemma 5.** *The optimal dam height increases only.*

*Proof.* See Appendix H.  $\square$

**Lemma 6.** *The optimal dam height increases at energy-critical points.*

*Proof.* See Appendix I.  $\square$

The battery must be charged once it is energy-critical, the following definitions state what is the energy-critical point and how it is charged in the optimal solution.

**Definition 5** (The energy-critical point). *If at time point  $t$  the energy in the battery available for transmitting the data is 0, then the time point  $t$  is an energy-critical point.*

Note that, at an energy-critical point, there is only a little energy that keeps the device functional remains and there's no energy available for transmitting the data.

Immediately following an optimal energy-critical point, there must be a charging phase with length at least length  $\Delta t$ , where  $\Delta t$  is the minimum time required for a device to stay harvesting which is imposed by the hardware.

**Definition 6** (The fast switching cycle and fast switching period). *A cycle is called the fast switching cycle if its charging phase is with length  $\Delta t$ , and the sending phase uses up all the energy in the battery. Adjacent fast switching cycles are called a fast switching period.*

Note that an example of the optimal solution that satisfies all the above Lemma 5, 6 and Definition 6 is given in Appendix J.

We are now ready to present the algorithm. The high level idea is quite simple, we want to find the first dam height changing point for the optimal dam height and after such a point, the same problem repeats. According to Lemma 6, 1) at such a point, the battery is energy-critical, and 2) before such a point, there is a single dam height, and 3) after such a point, the dam height increases. Hence, we find the largest dam height  $w$  for the entire duration that is feasible with an energy-critical point. We will prove later that such a point is the first optimal dam height changing point, and the dam height  $w$  is also optimal before such a point.

We can call the previously introduced `dam_raising_shotg` to directly return such a dam height  $w$ . Let the procedure of finding the energy-critical point for  $w$  be `find_emptyP( $t_s, t_e, E_0, w$ )`, where  $[t_s, t_e]$  is the duration in consideration,  $E_0$  is the initial energy for such duration, and  $w$  is the given dam height. The procedure returns the first energy-critical point  $\tau$  if it exists. Starting from  $\tau$ , we charge the battery for  $\Delta t$  time, and charge  $\int_{t=\tau}^{\tau+\Delta t} p(t) dt$  energy into the battery. The point  $\tau + \Delta t$  will be treated as the new starting point for the next iteration.

Algorithm `Varying_Source_WPT` computes all the changing points and the dam heights.

---

**Algorithm 2:** `Varying_Source_WPT`


---

```

1  $\tau_0 = 0, E_0 = E_{init};$ 
2 while  $\tau_0 < T$  do
3    $w = \text{dam\_raising\_shotg}(\tau_0, T, E_0);$ 
4    $\tau = \text{find\_emptyP}(\tau_0, T, E_0, w);$ 
5   Set dam height  $w$  in  $[\tau_0, \tau]$ ;
6    $\tau_0 = \tau + \Delta t, E_0 = \int_{t=\tau}^{\tau+\Delta t} p(t) dt;$ 
7 end

```

---

**Theorem 7.** *The algorithm `Varying_Source_WPT` computes the optimal schedule for the offline problem, and the time complexity of the algorithm is  $O(T^2 \log(\frac{\rho_{max}}{\Delta}) / \Delta t)$ .*

*Proof.* See Appendix K.  $\square$

An example of the execution of Algorithm `Varying_Source_WPT` is illustrated in Fig. 6. By line 3, we slowly raise the dam height  $w$  and the corresponding water table  $P_w(w)$ .

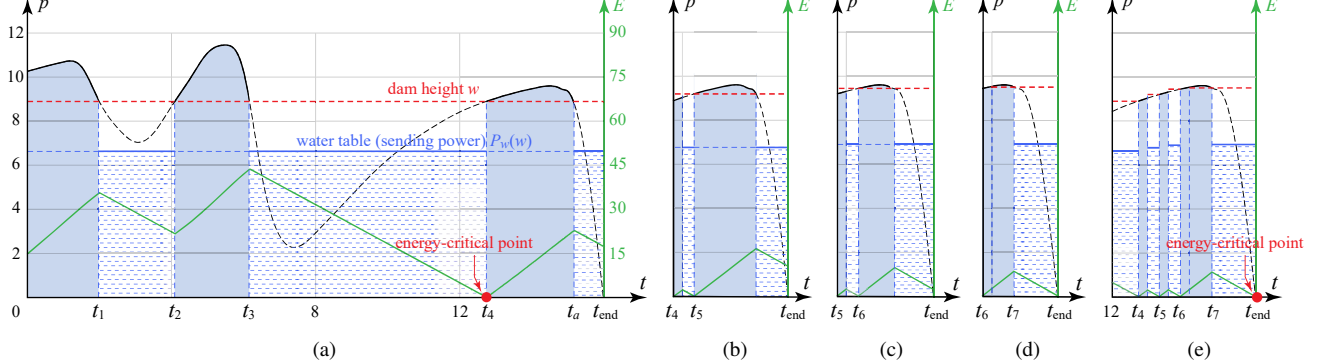


Fig. 6. The *dam raising system* may generate multiple dam heights. (a) The dam height  $w$  is slowly raised to the highest position that is feasible. In such a position, there must be an energy-critical point so that further raising will cause an energy shortage. The dam height before such a point is optimal. (b) Once the battery is energy-critical ( $t_4$  at (a)), we charge the battery for  $\Delta t$  time. Starting at this point, the same problem repeats. In this new problem, the remaining energy curve will not touch the x-axis until the dam continues to be raised above  $p(t_4)$ . This is called the fast switching cycle. (c) A number of adjacent fast switching cycles follow, and they are called the fast switching period. (d) When the dam continues to be raised above  $p(t_6)$ , the first energy-critical point that appears is  $t_{\text{end}}$ . Therefore, the fast switching period ended. (e) Full view of the fast switching period. The fast switching period begins at  $t_4$  and ends at  $t_6$ , and there are 2 fast switching cycles in the fast switching period:  $t_4 \sim t_5$  and  $t_5 \sim t_6$ .

As the dam height  $w$  grows larger, the green *remaining energy curve* increases less but decreases in a larger slope, as a result, this curve generally becomes lower in position. Once the dam height  $w$  is raised to a height that causes the curve to touch the x-axis, we stop, because that means the battery is energy-critical at the touch point. Line 3 returns this height  $w$  and line 4 returns the time of the touch point  $\tau$ . We have proved such dam height is optimal. Note that, since the battery is energy-critical at  $\tau$ , according to Definition 6, we set interval  $[\tau, \tau + \Delta t]$  to charge the battery, and the charged energy  $E_0 = \int_{t=\tau}^{\tau+\Delta t} p(t) dt$ . In Fig. 6(b), the *remaining energy curve* will not touch the x-axis until the dam height continues to rise above  $p(t_4)$ . Since the previous charging phase length  $\Delta t$  is small, the initial energy  $E_0 = \int_{t=\tau}^{\tau+\Delta t} p(t) dt$  is small, so with a small sending phase, the curve touches x-axis, and we stop. This is called the *fast switching cycle*, obviously, there will be fast switches in this period among harvesting and transmitting phases. The *fast switching period* may last for a number of more cycles, like in Fig. 6(c). In Fig. 6(d), when the dam continues to be raised above  $p(t_6)$ , the first energy-critical point that appears is  $t_{\text{end}}$ . Therefore, the fast switching period ended. Fig. 6(d) gives a full view of the fast switching period. The fast switching period starts from  $t_4$  and ends at  $t_6$ . There are 2 fast switching cycles in the period:  $t_4 \sim t_5$  and  $t_5 \sim t_6$ .

A more complicated example with three dam heights and two *fast switching periods* is given in Appendix J.

## VI. ONLINE ALGORITHM AND SIMULATIONS

In this section, we study the online *HTT-scheduling* problem, where the phase switching points and the transmission power are determined based on the past and current harvesting power, *i.e.*, any  $p(t)$  is not known until time  $t$ . We propose a heuristic algorithm, namely *dam guided online algorithm*, which is based on the optimal properties obtained from the offline problem. We then provide some basic theoretical analysis of this online algorithm. Finally, performance evaluation is conducted by comparisons with the optimal offline solutions.

### A. Online Algorithm

The core idea of *dam guided online algorithm* is to use the history average harvesting power to anticipate any unknown further harvesting power and compute the next charging-sending cycle based on the current harvesting power. Meanwhile, we do not want the next cycle to last too long, because harvesting power is time-varying and we have no future information. We want the cycle to be as short as possible.

More specifically, assume at the current time  $t$ , the charging power is  $p$  and the battery energy is  $E_r$ , while the history average charging power is  $\bar{p}$ . Suppose  $l_1$ ,  $l_2$ , and  $\rho$  are the lengths of the charging phase, sending phase, and the sending power respectively, which are to be determined by the online algorithm.

A total of  $(l_1 + l_2)\bar{p}$  energy is expected to be harvested on average in the next cycle if both phases are used for charging. If we set the sending power to be  $P_w(\bar{p})$  in the second phase, then compared with the both phase charging case, this sending phase not only costs  $l_2 P_w(\bar{p})$  energy in sending data, but also costs  $l_2 \bar{p}$  energy less charged into the battery. Therefore, the remaining energy is  $(l_1 + l_2)\bar{p} - (l_2 P_w(\bar{p}) + l_2 \bar{p}) = l_1 \bar{p} - l_2 P_w(\bar{p})$ , *i.e.*, the sum of both cost should be deducted.

As long as  $l_1$  and  $l_2$  are small enough, we can treat harvesting power as a constant, which is  $p$ . Then, the sending phase with length  $l_2$  costs  $l_2 P_w(\bar{p}) + l_2 p$  energy loss, including  $l_2 P_w(\bar{p})$  energy consumed and  $l_2 p$  energy less charged. We want the energy loss to equal to the expected energy harvesting, *e.g.*,  $(l_1 + l_2)\bar{p} = l_2(P_w(\bar{p}) + p)$  because the energy charged and energy consumed should equal in a long run. Therefore,  $l_1$  and  $l_2$  satisfies

$$\frac{l_2}{l_1 + l_2} = \frac{\bar{p}}{p + P_w(\bar{p})}. \quad (12)$$

Obviously, only if  $\frac{\bar{p}}{p + P_w(\bar{p})} < 1$ , then  $l_1 > 0$ . Hence, we set  $l_1 = 0$  and  $l_2 = \Delta t$  when  $\frac{\bar{p}}{p + P_w(\bar{p})} \geq 1$ . When  $\frac{1}{2} < \frac{l_2}{l_1 + l_2} < 1$ ,  $l_1$  is smaller than  $l_2$ , we hence set  $t_1 = \Delta t$  and compute  $l_2$  accordingly,  $l_2 = \frac{\bar{p}}{p + P_w(\bar{p}) - \bar{p}} \Delta t$ . When  $\frac{l_2}{l_1 + l_2} \leq \frac{1}{2}$ ,  $l_2$  is

TABLE I  
SUMMARY OF ONLINE SETTINGS TO  $l_1$  AND  $l_2$

$l_1$	$\frac{\bar{p}}{p+P_w(\bar{p})} \geq 1$	$\frac{1}{2} < \frac{\bar{p}}{p+P_w(\bar{p})} < 1$	$\frac{\bar{p}}{p+P_w(\bar{p})} \leq \frac{1}{2}$
$l_2$	$0$	$\Delta t$	$\frac{\bar{p}}{p+P_w(\bar{p})-\bar{p}} \Delta t$

smaller, hence we set  $l_2 = \Delta t$  and  $l_1 = \frac{p+P_w(\bar{p})-\bar{p}}{\bar{p}} \Delta t$ . These settings to  $l_1$  and  $l_2$  are summarized in Table I.

The Algorithm `dam_guided_online` presents the detailed pseudo code.

### B. The Basic Theoretical Analysis

The general idea of our basic theoretical analysis is, we take two general intervals and analysis the throughput and energy usage within both intervals. Assume the time-varying harvesting power function  $p(t)$ ,  $0 \leq t \leq T$  has the average power at  $\bar{p}$ , then the two taken intervals must also average to  $\bar{p}$ , otherwise, they are not general enough. Let them be called interval  $x$  and interval  $y$ , both with length  $L$ . If  $x$  and  $y$  both have harvesting powers equal to  $\bar{p}$ , then it is quite straightforward to check that the proposed online algorithm produces a solution with throughput equal to the offline optimal solution.

We therefore focus on the cases when harvesting power in the two intervals varies. Assume  $p(t)$  is bounded by  $p_{min} \leq p(t) \leq p_{max}$ ,  $0 \leq t \leq T$ , and  $p_{min} = (1 - \gamma)\bar{p}$  and  $p_{max} = (1 + \gamma)\bar{p}$ , where  $\gamma$  represents the deviation of variation. We study the case where the two taken intervals have the largest variation deviation of  $p(t)$  because the throughput and energy usage are affected the most. Without loss of generality, we assume the harvesting power  $p = (1 - \gamma)\bar{p}$  in interval  $x$  and  $p = (1 + \gamma)\bar{p}$  in interval  $y$ , and  $x$  is before  $y$ . We will show next the throughput and energy usage differences between a

---

#### Algorithm 3: `dam_guided_online`( $E_r$ , $t$ , $p$ )

---

```

1 Update the average harvesting power  $\bar{p}$ ;
2 if  $\frac{p+P_w(\bar{p})}{\bar{p}} \leq 1$  then
3    $l_1 = 0$ ;
4    $l_2 = \Delta t$ ;
5 else if  $1 < \frac{p+P_w(\bar{p})}{\bar{p}} \leq 2$  then
6    $l_1 = \Delta t$ ;
7    $l_2 = \frac{\bar{p}}{p+P_w(\bar{p})-\bar{p}} \Delta t$ ;
8 else if  $2 < \frac{p+P_w(\bar{p})}{\bar{p}}$  then
9    $l_1 = \frac{p+P_w(\bar{p})-\bar{p}}{\bar{p}} \Delta t$ ;
10   $l_2 = \Delta t$ ;
11 end
12 if  $E_r + l_1 p - l_2 P_w(\bar{p}) < 0$  then
13    $l_2 = 0$ ;
14 end
15 Set charging phase  $[t, t + l_1]$ ;
16 Set sending phase  $[t + l_1, t + l_1 + l_2]$ , and sending
   power  $P_w(\bar{p})$ ;

```

---

simple offline solution and the online solution by the proposed online algorithm.

Assume in an offline solution, all energy harvested is used up in  $x$  and  $y$ , respectively, that is

$$E^{off} = 0.$$

Then, according to the constant harvesting power analysis in Section III and Eq. (7), we have the throughput for this offline solution as follows,

$$\begin{aligned} B^{off} &= (1 - \gamma)\bar{p}L \frac{\log(1 + P_w((1 - \gamma)\bar{p}))}{(1 - \gamma)\bar{p} + P_w((1 - \gamma)\bar{p})} \\ &\quad + (1 + \gamma)\bar{p}L \frac{\log(1 + P_w((1 + \gamma)\bar{p}))}{(1 + \gamma)\bar{p} + P_w((1 + \gamma)\bar{p})}. \end{aligned} \quad (13)$$

Since function  $B^{on}(p) = pL \frac{\log(1 + P_w(p))}{p + P_w(p)}$  is a concave function, so according to Jensen's inequality, we have

$$B^{off} \leq 2\bar{p}L \frac{\log(1 + P_w(\bar{p}))}{\bar{p} + P_w(\bar{p})}. \quad (14)$$

We now study the throughput and energy usage of the online solution produced by the proposed online algorithm. Since the online algorithm produces cycles with very small lengths, we first investigate the length percentage of both phases. Since the sending phase length percentage has already been presented in Eq. (12), the charging phase length percentage is therefore  $\frac{l_1}{l_1+l_2} = 1 - \frac{\bar{p}}{p+P_w(\bar{p})}$ . Therefore, we have

$$\frac{l_{x1}}{l_{x1} + l_{x2}} = 1 - \frac{\bar{p}}{(1 - \gamma)\bar{p} + P_w(\bar{p})}, \quad l_{x1} + l_{x2} = L$$

$$\frac{l_{y1}}{l_{y1} + l_{y2}} = 1 - \frac{\bar{p}}{(1 + \gamma)\bar{p} + P_w(\bar{p})}, \quad l_{y1} + l_{y2} = L$$

Therefore,

$$l_{x2} = \frac{\bar{p}}{(1 - \gamma)\bar{p} + P_w(\bar{p})}L$$

$$l_{y2} = \frac{\bar{p}}{(1 + \gamma)\bar{p} + P_w(\bar{p})}L$$

The throughput of the solution by our online algorithm is the sum of all data sent in every sending phase in both intervals  $x$  and interval  $y$ .

$$\begin{aligned} B^{on} &= l_{x2} \log(1 + P_w(\bar{p})) + l_{y2} \log(1 + P_w(\bar{p})) \\ &= \frac{\bar{p}}{(1 - \gamma)\bar{p} + P_w(\bar{p})}L \log(1 + P_w(\bar{p})) \\ &\quad + \frac{\bar{p}}{(1 + \gamma)\bar{p} + P_w(\bar{p})}L \log(1 + P_w(\bar{p})). \end{aligned}$$

Since function  $B^{on}(p) = \bar{p}L \frac{\log(1 + P_w(p))}{p + P_w(p)}$  is a concave function, so

$$B^{on} \geq 2\bar{p}L \frac{\log(1 + P_w(\bar{p}))}{\bar{p} + P_w(\bar{p})}. \quad (15)$$

Therefore,

$$B^{on} \geq B^{off}. \quad (16)$$

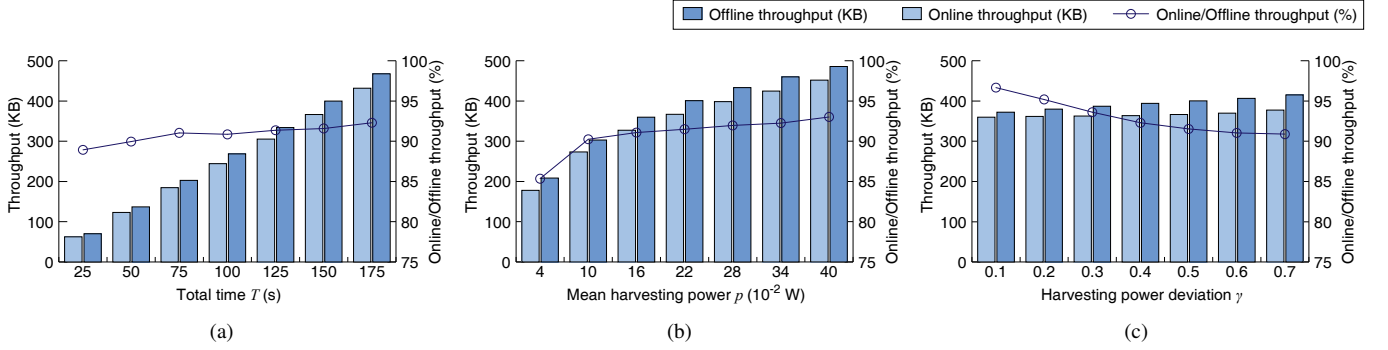


Fig. 7. The achieved throughput by the online algorithm to the offline optimal throughput. The default setting is total time  $T = 150$ s, the mean harvesting power  $\hat{p} = 0.22$ W, and the harvesting power deviation  $\gamma = 0.5$ . In (a), the total time slot  $T$  varies from 25s to 175s, with a step of 25s. In (b), the mean harvesting power  $\hat{p}$  varies from 0.04W to 0.4W with a step of 0.06W. In (c), the harvesting power deviation  $\gamma$  varies from 0.1 to 0.7 with a step of 0.1.

The energy harvested into the system by our online algorithm in charging phases of both  $x$  and  $y$  is

$$\begin{aligned} E_{in}^{on} &= \left(1 - \frac{\bar{p}}{(1-\gamma)\bar{p} + P_w(\bar{p})}\right)L(1-\gamma)\bar{p} \\ &\quad + \left(1 - \frac{\bar{p}}{(1+\gamma)\bar{p} + P_w(\bar{p})}\right)L(1+\gamma)\bar{p} \\ &= L\bar{p}\left(\frac{(1-\gamma)(1-\gamma\frac{\bar{p}}{P_w(\bar{p})})}{(1-\gamma)\frac{\bar{p}}{P_w(\bar{p})}+1} + \frac{(1+\gamma)(1+\gamma\frac{\bar{p}}{P_w(\bar{p})})}{(1+\gamma)\frac{\bar{p}}{P_w(\bar{p})}+1}\right). \end{aligned}$$

The energy consumed in the sending phases of both intervals is

$$\begin{aligned} E_{out}^{on} &= \frac{\bar{p}}{(1-\gamma)\bar{p} + P_w(\bar{p})}LP_w(\bar{p}) \\ &\quad + \frac{\bar{p}}{(1+\gamma)\bar{p} + P_w(\bar{p})}LP_w(\bar{p}) \\ &= L\bar{p}\left(\frac{1}{(1-\gamma)\frac{\bar{p}}{P_w(\bar{p})}+1} + \frac{1}{(1+\gamma)\frac{\bar{p}}{P_w(\bar{p})}+1}\right). \end{aligned}$$

So,

$$\begin{aligned} E^{on} &= E_{in}^{on} - E_{out}^{on} = L\bar{p}\left(\frac{-\gamma - \gamma\frac{\bar{p}}{P_w(\bar{p})} + \gamma^2\frac{\bar{p}}{P_w(\bar{p})}}{(1-\gamma)\frac{\bar{p}}{P_w(\bar{p})}+1} \right. \\ &\quad \left. + \frac{\gamma + \gamma\frac{\bar{p}}{P_w(\bar{p})} + \gamma^2\frac{\bar{p}}{P_w(\bar{p})}}{(1+\gamma)\frac{\bar{p}}{P_w(\bar{p})}+1}\right) = 0 = E^{off}. \end{aligned}$$

In conclusion, our online algorithm produces a solution that delivers more data than a simple offline solution using the same amount of energy, *i.e.*,  $B^{on} \geq B^{off}$  and  $E^{on} = E^{off}$ . Besides, if the harvesting power  $p(t)$  is a constant and not allowed to change, *i.e.*,  $\gamma = 0$ , then our online algorithm generates exactly the same solution as the offline optimal solution, *i.e.*,  $B^{on} = B^{off}$ .

### C. Simulations

In this subsection, the proposed `dam_guided_online` algorithm is implemented and its efficiency is investigated through simulations. In this evaluation, we compare the performance of the proposed online algorithm against the optimal offline solution. We also compare the performance of the proposed algorithm against the time-sharing algorithm. Note that the throughput of the optimal offline solution is the upper

bound any online algorithm can ever achieve. A desired online solution is very close to the optimal offline solution.

In simulations, we assume there exists some small time interval length, in which the harvesting power does not change. We call such a small time interval a time slot. A total of  $T$  time slots are considered in evaluating the proposed algorithm, by default  $T = 150$ s. For all time slots, the harvesting power is assumed to be a random variable following the uniform distribution  $U((1-\gamma)\hat{p}, (1+\gamma)\hat{p})$ , with the default mean harvesting power  $\hat{p} = 0.22$ W, and default harvesting power deviation  $\gamma = 0.5$ .

In this simulation, we change the total time slot  $T$ , the mean harvesting power  $\hat{p}$ , and the harvesting power deviation  $\gamma$ , one at a time, to evaluate their impact on the algorithm performance, as in [27]. Each value shown in the figures of this section is the mean value of simulation results from 20 random instances, and in each instance, a total of  $T$  harvesting powers are generated according to the above model.

The ratio that the online algorithm achieves the offline maximum throughput is illustrated in Fig. 7, where the throughput of our online algorithm is compared to the offline optimal solution that maximizes the throughput.

In Fig. 7(a), the total time slot  $T$  varies from 25s to 175s, with a step of 25s. We can see that as the total time  $T$  increase, the throughput increases as well. Meanwhile, the larger the total time slots, the better our online algorithm performance. This is because the heart of our online algorithm is to accurately anticipate future powers, and we use the history average harvesting power. For more time slots, the more accurate the history average is in prediction. However, even if the total time slot is only 25s, the achieved ratio is nearly 88%, and for larger total time, the achieved ratio is around 92%.

In Fig. 7(b), the mean harvesting power  $\hat{p}$  varies from 0.04W to 0.4W with a step of 0.06W. We can see that both the throughput and the efficiency of the proposed algorithm increase as the mean harvesting power  $\hat{p}$  increases. This is because when  $\hat{p}$  goes smaller, more time is needed to harvest the same amount of energy. As a result, more difficulty should be faced for our heuristic algorithm to achieve a good throughput, so its efficiency drops. However, in all tested cases, the achieved ratio stays higher than 85%.

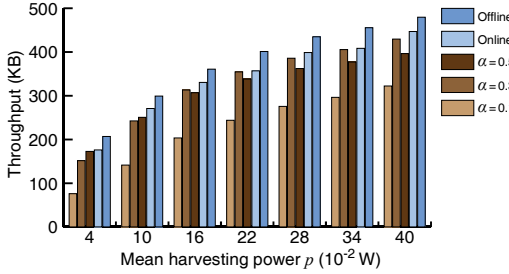


Fig. 8. The achieved throughput by the time-sharing algorithm ( $\alpha = 0.1$ ,  $\alpha = 0.3$ ,  $\alpha = 0.5$ ), proposed online algorithm and proposed offline algorithm. The default setting is total time  $T = 150$ s and the harvesting power deviation  $\gamma = 0.5$ . The mean harvesting power  $\hat{p}$  varies from  $0.04\text{W}$  to  $0.4\text{W}$  with a step of  $0.06\text{W}$ .

In Fig. 7(c), the harvesting power deviation  $\gamma$  varies from 0.1 to 0.7 with a step of 0.1. The throughput of our online algorithm stays approximately the same while the offline algorithm increases as the deviation  $\gamma$  increases. This is because the larger the deviation, the more difficult it is to predict the further harvesting power. Therefore, our method based on the historical average becomes less efficient. However, we can see from the figure that even if the deviation is as high as 0.7, our online algorithm can achieve around 90% ratio.

The comparison of the proposed online and offline algorithm between time-sharing algorithm is illustrated in Fig. 8, where the mean harvesting power  $\hat{p}$  varies from  $0.04\text{W}$  to  $0.4\text{W}$  with a step of  $0.06\text{W}$ . The time-sharing algorithm is borrowed from [28], which simply divides each time slot into the harvesting period and sending period. The ratio of harvesting period to time slot is  $\alpha$ . We here compared the throughput of the time-sharing algorithm and the optimal online and offline algorithm we proposed. We can see from the figure that in every situation, our algorithm achieved higher throughput than the time-sharing algorithm.

As a conclusion of the simulation, the proposed online algorithm is efficient and achieves more than 90% of the offline maximum throughput in most tested cases. Both the online algorithm and offline algorithm overcome the time-sharing algorithm.

## VII. CONCLUSIONS AND FUTURE WORKS

In this paper, we first formulated the throughput maximization *HTT-scheduling* problem for the time-varying RF energy harvesting systems. Then the *wopt* power was introduced, which is with a basic but important property. Based on this property, we introduced the concept of the *dam height*. We then investigated a special case of the problem, *e.g.*, the harvesting power is monotonically decreasing. Some optimality properties were observed, and the *dam raising system* was designed to solve the special case problem. These properties and the *dam raising system* were then extended to the general scenario, where the harvesting power can change dynamically. Finally, an online heuristic algorithm was proposed and simulations were conducted to evaluate its efficiency.

Our future work will focus on extending the system model and optimization framework to scenarios involving multiple

wireless transmitters and receivers. This direction will address interference and distributed resource allocation in networked environments, thereby broadening the applicability of our results to more realistic deployment conditions.

## APPENDIX

### A. Proof of Theorem 2

Actually, Theorem 2 is a special case of Theorem 5 when the  $p(t)$  is monotonically decreasing. Therefore, we will prove Theorem 2 briefly, focusing our main efforts on the proof of Theorem 5.

Theorem 2 can be succinctly summarized in the following point: there is a dam height  $w$ , such that higher harvesting power duration harvests energy and lower power duration transmits data. This is because, otherwise, we can identify a very small charging interval  $[a, a + \delta]$  and a sending interval  $[b, b + \delta]$  with an equal length such that function  $p(t)$  at any point in  $[a, a + \delta]$  is smaller than the function at any point in  $[b, b + \delta]$ . Because the harvesting power  $p(t)$  is decreasing, we must have the charging interval  $[a, a + \delta]$  after the sending interval  $[b, b + \delta]$ . Then, we can swap the two operations for the two intervals. By doing so, we move to charge the battery earlier and larger, therefore the throughput can be increased in the sending phase.

### B. Proof of Theorem 3

Actually, Theorem 3 is a special case of Theorem 6 when the  $p(t)$  is monotonically decreasing. Therefore, we will therefore prove Theorem 3 briefly, focusing our main efforts on the proof of Theorem 6.

Theorem 3 can be succinctly summarized in the following point: the sending power is  $P_w(w)$  in any sending phase, where  $w$  is the dam height that distinguishes charging phases from sending phases. Because the harvesting power  $p(t)$  decreases, there is only one (energy harvesting, data transmission) cycle, *i.e.*, one charging phase and one sending phase. Suppose  $t_1$  is the phase switching point, then  $p(t_1) = w$ . Since  $p(t)$  is a continuous function, we can treat the harvesting power in  $[t_1 - \delta, t_1 + \delta]$  as a constant  $w$ , as long as  $\delta$  is small enough. If the sending power  $P_w(w) < \rho$  ( $P_w(w) > \rho$ ), then, by Lemma 3, interval  $[t_1 - \delta, t_1]$  ( $[t_1, t_1 + \delta]$ ) can be included into (excluded from) the only sending phase, to improve the throughput. Hence, we must have the sending power  $\rho = P_w(w)$ .

### C. Proof of Theorem 4

First, we prove that the algorithm can compute the optimal HTT schedule of decreasing harvesting power. From Lemma 2 we could know that as dam height increases, the throughput monotonically increases and the remaining energy monotonically decreases. Thus, the HTT schedule of decreasing harvesting power is monotonic. Since monotonic problems can definitely be solved using bisection method, the algorithm can give optimal HTT schedule of decreasing harvesting power.

Next, we prove that the algorithm has a time complexity of  $O(T \cdot \log(\frac{\rho_{max}}{\Delta}))$ . When the algorithm returns at Line 11,

we must have  $w_{upper} - w_{lower} < \Delta$ . We know that after each iteration, the value  $w_{upper} - w_{lower}$  is reduced to its half. Therefore, after  $n$  iterations, we have  $w_{upper} - w_{lower} = \frac{1}{2^n}w_{max}$ . Therefore, when the algorithm returns at Line 11, we have  $\frac{1}{2^n}w_{max} < \Delta$ , which could be equivalently written as  $n > \log_2(\frac{w_{max}}{\Delta})$ . Note that in each iteration, we invoke `is_shortage` for  $O(T)$  times. So, the overall time complexity is  $O(T \cdot \log(\frac{w_{max}}{\Delta}))$ .

#### D. Proof of Theorem 5

We prove this theorem by contradiction. In the optimal schedule, assume, for contradictory, there does not exist time  $\tau_i$  and power level  $w_i$  for interval  $[\tau_{i-1}, \tau_i]$  such that in the interval any charging phase has  $p(t) > w_i$  and any sending phase has  $p(t) \leq w_i$ , then, we claim there is at least one sending phase has different  $p(t)$  on its both ends. The core idea of our method is to show such a schedule can be further improved, contradicting to its optimality assumption.

There are only two situations where the  $p(t)$  on both ends of the sending phase are not equal: the right end is higher, or the left end is higher. Let's call the situation where the right end is higher the “left low, right high” and the situation where the left end is higher the “left high, right low”, which are shown in Fig. 9 and 10.

We first consider the “left low, right high” situation, which is shown in Fig. 9(a). Suppose the sending phase is  $t_1 \sim t_2$  and  $p(t_1) < p(t_2)$  and the sending power is  $\rho$ . Suppose  $E(t_2) = C$ , where  $C$  is a constant and  $C \geq 0$ . Therefore, we have:

$$E(t_0) + \int_{t_0}^{t_1} p(t) dt - \rho(t_2 - t_1) = C. \quad (17)$$

The first step is to move  $t_1$  and  $t_2$  forward, which is shown in Fig. 9(b). We move  $t_1$  and  $t_2$  forward to  $t_3$  and  $t_4$ . In this process we keep  $E(t_4) = C$ , until we find a pair of  $(t_3, t_4)$  such that  $p(t_3) = p(t_4)$ . We could always find  $(t_3, t_4)$ , unless  $t_3$  touches the start point, which turned out to be a fast-switching cycle. Note that the sending power is still  $\rho$  here. Because  $t_1 = t_3 + (t_1 - t_3)$ , Eq. (17) could also be written as:

$$E(t_0) + \int_{t_0}^{t_3} p(t) dt + \int_{t_3}^{t_1} p(t) dt - \rho(t_2 - t_1) = C. \quad (18)$$

The second step is to find  $t_5$ , which is shown in Fig. 9(c). We need to find  $t_5$  between  $t_4$  and  $t_2$  such that  $E(t_N)$  remains the same because  $E(t_N)$  is different between Fig. 9(a) and Fig. 9(b). Therefore, we have:

$$E(t_0) + \int_{t_0}^{t_3} p(t) dt + \int_{t_4}^{t_5} p(t) dt - \rho(t_4 - t_3) - \rho(t_2 - t_5) = C. \quad (19)$$

Subtract Eq. (18) from Eq. (19) and we have:

$$\int_{t_4}^{t_5} p(t) dt - \int_{t_3}^{t_1} p(t) dt = \rho(t_1 - t_3) - \rho(t_5 - t_4). \quad (20)$$

We claim that  $t_5 - t_4$  must no greater than  $t_1 - t_3$ . Otherwise, we will find that, comparing Fig. 9(a) with Fig. 9(c), more energy is charged and less energy is used, however, the remaining energy stays the same, which is a contradiction. The details of the proof are as follows:

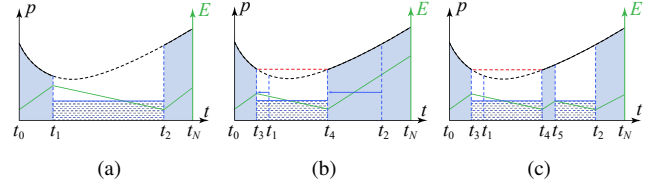


Fig. 9. The process of improving the throughput of the “left low, right high” situation.

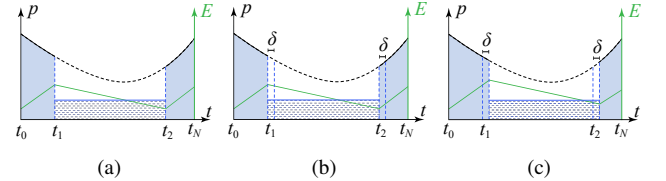


Fig. 10. The process of improving the throughput of the “left high, right low” situation.

Suppose  $t_5 - t_4 > t_1 - t_3$ . Add  $t_2$  on both sides so

$$t_2 + t_5 - t_4 > t_2 + t_1 - t_3.$$

Move  $t_5 - t_4$  and  $t_1$  to opposite side, and we have

$$t_2 - t_1 > t_2 - t_5 + t_4 - t_3.$$

The left part of the inequality is the length of the sending phase in Fig. 9(a) and the right part is the length of sending phases in Fig. 9(c). Note that the sending power is always  $\rho$ . Therefore, the energy used to send in Fig. 9(a) is larger than that in Fig. 9(c).

Meanwhile, from Fig. 9(c) we could find that  $p(t)$  is larger in  $t_4 \sim t_5$  than that in  $t_3 \sim t_1$ . Note that  $t_5 - t_4$  is also greater than  $t_1 - t_3$ . Therefore, we have

$$\int_{t_4}^{t_5} p(t) dt > \int_{t_3}^{t_1} p(t) dt$$

Add  $\int_{t_0}^{t_3} p(t) dt$  on both sides, and we get:

$$\int_{t_0}^{t_3} p(t) dt + \int_{t_4}^{t_5} p(t) dt > \int_{t_0}^{t_3} p(t) dt + \int_{t_3}^{t_1} p(t) dt$$

which could be also written as

$$\int_{t_0}^{t_3} p(t) dt + \int_{t_4}^{t_5} p(t) dt > \int_{t_0}^{t_1} p(t) dt.$$

The right part of the inequality is the harvested energy in Fig. 9(a) and the left part is the harvested energy in Fig. 9(c). Therefore, the energy harvested in Fig. 9(a) is less than that in Fig. 9(c). Therefore, the relationship of harvested energy between Fig. 9(a) and Fig. 9(c) contradicts the relationship of sending-used energy between Fig. 9(a) and Fig. 9(c). Therefore,  $t_5 - t_4$  must no greater than  $t_1 - t_3$ .

Add  $t_2$  on both sides of  $t_5 - t_4 \leq t_1 - t_3$ , and we have

$$t_2 + t_5 - t_4 \leq t_2 + t_1 - t_3.$$

Move  $t_5 - t_4$  and  $t_1$  to opposite side, and we have

$$t_2 - t_1 \leq t_2 - t_5 + t_4 - t_3.$$

The left part of the inequality is the length of the sending phase in Fig. 9(a) and the right part is the length of the sending phases in Fig. 9(c). Note that the sending power is always  $\rho$ . Therefore, the sending rate is always a constant, which is  $\log(1 + \rho)$ . Therefore, the throughput in Fig. 9(c) is no less than that in Fig. 9(a). Therefore, we improved the throughput of the “left low, right high” situation.

Next, we consider the “left high, right low” situation, which is shown in Fig. 10(a). Suppose the sending phase is  $t_1 \sim t_2$ ,  $p(t_1) > p(t_2)$ , and sending power is  $\rho$ . We continuously perform the following operations until  $p(t_1) = p(t_2)$ .

First, we select a short interval of  $\delta$  after  $t_1$  and  $t_2$ , which is shown in Fig. 10(b).  $\delta$  must satisfy the following condition: every  $p(t)$  in  $t_1 \sim t_1 + \delta$  must be greater than that in  $t_2 \sim t_2 + \delta$ . Therefore, we have:

$$\int_{t_1}^{t_1+\delta} p(t) dt > \int_{t_2}^{t_2+\delta} p(t) dt.$$

That is to say, the harvested energy in  $t_1 \sim t_1 + \delta$  is larger than that in  $t_2 \sim t_2 + \delta$ . Then we swap these two intervals, which is shown in Fig. 10(c). Swapping is always feasible. Because by swapping, we first harvest and then send. After swapping, the remaining energy at  $t_2 + \delta$  should be larger than 0 because the harvested energy in  $t_1 \sim t_1 + \delta$  is larger than that in  $t_2 \sim t_2 + \delta$ . The excess remaining energy could be used to increase sending power in the sending phase. Therefore, the throughput could be improved.

By continuously perform these operations,  $p(t_1)$  will eventually equal to  $p(t_2)$ . Therefore, we improved the throughput of the “left high, right low” situation.

Therefore, the  $p(t)$  on both ends of the sending phase should be the same, otherwise, we can always improve.

### E. Proof of Lemma 3

Here we draw Fig. 11 to show how we expand and shrink. Below we prove the existence of the operation.

We first consider the situation of shrinking, which is shown in Fig. 11(a). Suppose the original dam height is  $w$ . Therefore, according to Eq. (8), the optimal sending power is  $P_w(w)$ . Suppose the actually sending power is  $\rho$ , and  $P_w(w) > \rho$ .

Assume we exclude a small duration of  $\delta_1$  at the beginning and exclude  $\delta_2$  at the end. Note that after we shrink, both ends are still at the same height  $w'$ . Here we use  $E_1$  to represent the energy consumed in the sending period before we shrink and  $E_2$  represents that after we shrink. Therefore, we have

$$E_1 = -\rho l$$

$$E_2 = \int_{\delta_1} p(t) dt + \int_{\delta_2} p(t) dt - (l - \delta_1 - \delta_2)P_w(w')$$

Assume  $\Delta E$  is the difference of energy consumption between the schedules before and after we shrink. Therefore, we have:

$$\begin{aligned} \Delta E &= E_2 - E_1 \\ &= \int_{\delta_1} p(t) dt + \int_{\delta_2} p(t) dt + (l\rho - (l - \delta_1 - \delta_2)P_w(w')). \end{aligned}$$

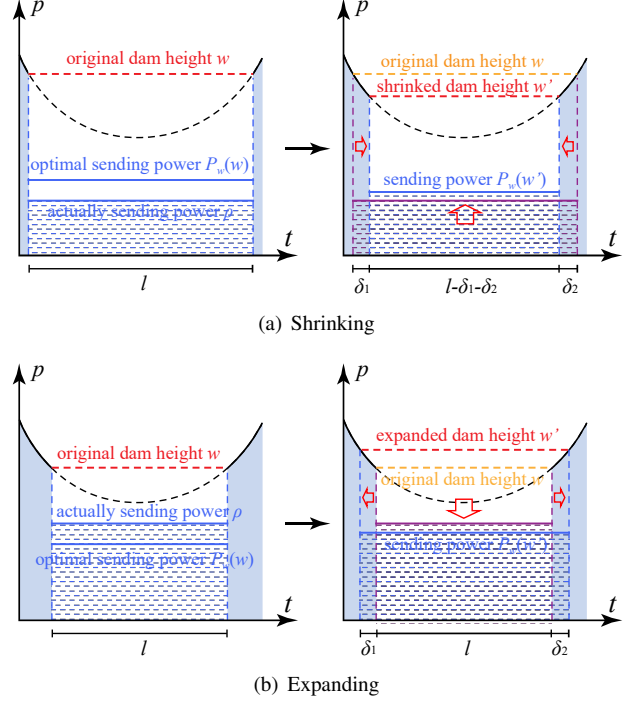


Fig. 11. If actually sending power  $\rho$  is smaller (larger) than the optimal sending power  $P_w(w)$ , we can expand (shrink) the sending phase to improve the solution.

When  $\delta_1 + \delta_2 = l$ , we have:

$$\Delta E = \int_{\delta_1} p(t) dt + \int_{\delta_2} p(t) dt + \rho l > 0.$$

When  $\delta_1 + \delta_2 = 0$ , which means  $w = w'$ , we have:

$$\Delta E = l(\rho - P_w(w')) = l(\rho - P_w(w)) < 0.$$

Note that  $\Delta E$  is a continuous function of  $\delta_1$  and  $\delta_2$ . Therefore, according to Bolzano’s Theorem there exists a pair of  $(\delta_1, \delta_2)$  which let  $\Delta E = 0$ . Therefore, there exists an operation that meets the first constraint.

Next, we prove this operation meets the second constraint, which means the operation doesn’t decrease the throughput. Compared with the case before we shrink, the harvested energy that can be used in sending is  $\int_{\delta_1} p(t) dt + \int_{\delta_2} p(t) dt$  more. Let  $\delta = \delta_1 + \delta_2$  and  $\rho' = P_w(w')$ . Note that

$$\int_{\delta_1} p(t) dt + \int_{\delta_2} p(t) dt > w'(\delta_1 + \delta_2) = w'\delta.$$

Let’s ignore the difference between  $\int_{\delta_1} p(t) dt + \int_{\delta_2} p(t) dt$  and  $w'\delta$ , because if we don’t decrease throughput with less energy, we won’t decrease the throughput with more energy.

Suppose we used  $E$  energy before we shrink. We have  $E + w'l = \rho l + w'l$ , hence  $l = \frac{E+w'l}{w'+\rho}$ , and therefore

$$B = (E + w'l) \frac{\log(1 + \rho)}{w' + \rho}. \quad (21)$$

After we shrink, we have

$$\rho'(l - \delta) = E + w'\delta.$$

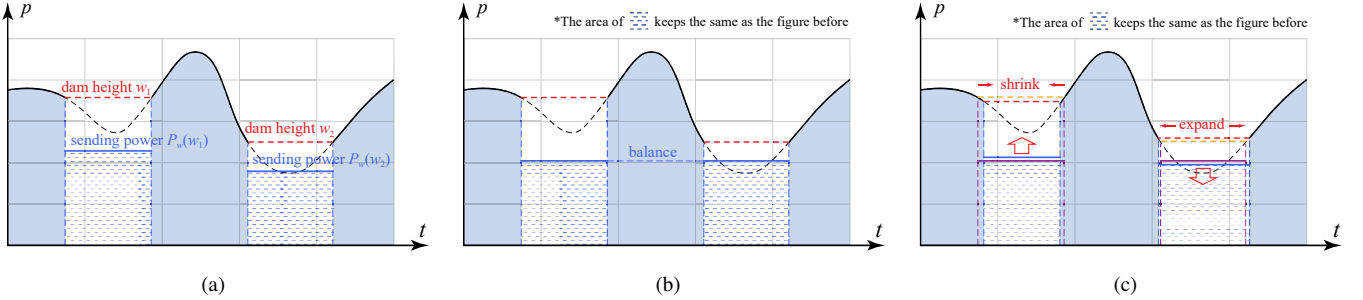


Fig. 12. The process of improving throughput while not increasing energy consumption. (a) A common situation where has two different dam heights. (b) The balance operation. (c) The shrinking and expanding operation.

We have  $(w' + \rho')(l - \delta) = E + w'\delta - w'\delta + w'l$ , hence  $l - \delta = \frac{E + w'l}{w' + \rho'}$ , and therefore

$$B' = (E + w'l) \frac{\log(1 + \rho')}{w' + \rho'}. \quad (22)$$

By treating  $\rho$  as a variable, the throughput is a function of  $\rho$ . Through the analysis of Eq. (7) and the Fig. 3, we can easily conclude that when  $P_w(w') > \rho' \geq \rho$ , we have  $B' \geq B$ . Therefore, this operation meets the second constraint.

The proof of expanding is the same as shrinking, which will not be further elaborated here.

#### F. Proof of Theorem 6

We will use Lemma 3 (Expanding and shrinking) to prove Theorem 6 here. Suppose there is a sending phase in the optimal HTT schedule where sending power  $\rho$  is not  $P_w(w)$ .  $w$  is the dam height of the sending phase. According to Lemma 3, the shrinking(expanding) doesn't change the energy consumption. Moreover, the shrinking(expanding) will not decrease the throughput. Therefore, we could apply shrinking(expanding) on the sending phase. And the throughput after we apply shrinking(expanding) will be no less than that before. Therefore, we improved the optimal HTT schedule, which is a contradiction. Therefore, in each sending phase of the optimal HTT schedule, the sending power should be  $P_w(w)$ , where  $w$  is the dam height of the sending phase.

#### G. Proof of Lemma 4

Consider a common situation shown in the Fig. 12(a). Assume there are two sending phases. The dam heights and sending power of these two sending phases are  $w_1$ ,  $w_2$  and  $P_w(w_1)$ ,  $P_w(w_2)$ . Note that  $w_1 \neq w_2$ . By performing the following operations, we could improve the throughput without increasing energy consumption.

First we balance the sending power of two sending phases, which is shown in Fig. 12(b). Suppose the lengths of two sending phases are  $l_1$  and  $l_2$ . For the sake of convenience in our proof, let  $\rho_1 = P_w(w_1)$ ,  $\rho_2 = P_w(w_2)$  and denote  $\rho_3$  as the balanced sending power. The premise of the balance operation is not to increase energy consumption, which means the areas of sending phases are equal in Fig. 12(a) and Fig. 12(b). Thus,

$$\rho_1 l_1 + \rho_2 l_2 = \rho_3 (l_1 + l_2).$$

Therefore,

$$\rho_3 = \frac{\rho_1 l_1 + \rho_2 l_2}{l_1 + l_2}. \quad (23)$$

Before we perform the balance operation, the throughput is  $l_1 \log(1 + \rho_1) + l_2 \log(1 + \rho_2)$ . After we perform the operation, the throughput is  $(l_1 + l_2) \log(1 + \rho_3)$ . Because the concavity of the *power-rate* function, we could use the Jensen's inequality. Thus, we have

$$\frac{l_1 \log(1 + \rho_1) + l_2 \log(1 + \rho_2)}{l_1 + l_2} < \log\left(1 + \frac{\rho_1 l_1 + \rho_2 l_2}{l_1 + l_2}\right). \quad (24)$$

By substituting Eq. (23) into Eq. (24), we can get

$$l_1 \log(1 + \rho_1) + l_2 \log(1 + \rho_2) < (l_1 + l_2) \log(1 + \rho_3). \quad (25)$$

Note that the left part of Eq. (25) is the throughput before the operation and the right part is the throughput after the operation. Therefore, the balance operation improves the throughput without increasing energy consumption.

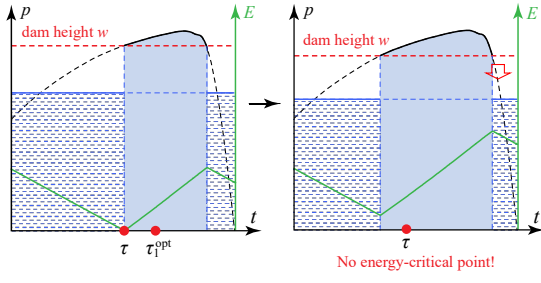
Next, we perform shrinking and expanding operations in two sending phases. According to the Lemma 3, both the shrinking and expanding operations do not increase the energy consumption and both the operations do not decrease the throughput. Therefore, the throughput is improved without increasing energy consumption after we perform these two operations in the sending phases.

Note that after performing operations shown in Fig. 12(b) and Fig. 12(c), the difference between  $w_1$  and  $w_2$  decreased. This is because the shrinking(expanding) operation shortened the length of the left(right) sending phase. Therefore, the dam height of the left(right) sending phase in Fig. 12(c) decreased(increased) compared with Fig. 12(a). Thus, the difference between  $w_1$  and  $w_2$  decreased.

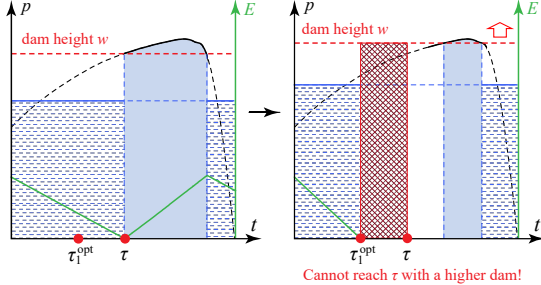
By continuously performing operations in Fig. 12(b) and Fig. 12(c), the dam heights of the two sending phases will eventually reach the same height. In this process, the throughput was improved while the energy consumption was not increased.

#### H. Proof of Lemma 5

Suppose otherwise, the optimal dam height decreases at time instance  $\tau_i$ , from  $w_i$  to  $w_{i+1}$ , while  $w_i > w_{i+1}$ . We can apply Lemma 4 to find a shared dam height  $w$  for  $[\tau_{i-1}, \tau_{i+1}]$ . Switch to use  $w$  is always feasible because  $w_i > w > w_{i+1}$ ,



(a)  $\tau_1^{opt} > \tau$ . After we lowered the dam, we couldn't find any energy-critical point. This contradicts  $\tau_1^{opt}$ .



(b)  $\tau_1^{opt} < \tau$ . After raising the dam, we need to reach  $\tau$  with a higher dam height according to Lemma 5. However, this is impossible.

Fig. 13. If  $\tau_1^{opt} \neq \tau$ , then there are two cases:  $\tau_1^{opt} > \tau$  and  $\tau_1^{opt} < \tau$ .

which means some energy originally used before  $\tau_i$  is now saved in battery and used after  $\tau_i$ . However, according to Lemma 4, the new dam height transmits more data using the same amount of energy. This is a contradiction.

### I. Proof of Lemma 6

Suppose otherwise, the optimal dam height increases at time instance  $\tau_i$ , but  $R(t_i) > 0$ . By Lemma 4, we can increase  $w_i$  and decrease  $w_{i+1}$  to improve data transmission using the same amount of energy before  $\tau_{i+1}$ . As long as  $R(t_i) \geq 0$  after the modification, there is no violation of the *battery constraint*, which is a contradiction.

### J. An example of the optimal solution

An example of the optimal solution that satisfy Lemma 5, 6, and Definition 6 is given in Fig. 14.

### K. Proof of Theorem 7

First, we prove that the algorithm can compute the optimal HTT schedule for the offline problem. In every iteration of the **while** loop, the same problem repeats, that is starting from  $\tau_0$ , find the next optimal changing point and the corresponding dam height. We, therefore, need only to show that in the first iteration, where  $\tau_0 = 0$ , the dam height  $w$  and changing time  $\tau$  are optimally set in Line 5, i.e.,  $\tau_1^{opt} = \tau$  and  $w_1^{opt} = w$ . Here we prove it by employing proof by contradiction.

Suppose, on the contrary, the first optimal changing point  $\tau_1^{opt} \neq \tau$ , where  $\tau$  is returned by `find_emptyP`. We then have the following two cases: (1)  $\tau_1^{opt} > \tau$  and (2)  $\tau_1^{opt} < \tau$ .

Case  $\tau_1^{opt} > \tau$ , illustrated in Fig. 13(a). We must have  $w_1^{opt} < w$  because the dam height  $w$  already makes the battery energy-critical at  $\tau$ , we have to lower the dam to make the energy-critical at  $\tau_1^{opt}$ . Since  $w$  returned by `dam_raising_shotg` is the highest feasible dam height position  $w$  and the battery is energy-critical at time  $\tau$  for the first time, then, for dam height lower than  $w$ , there doesn't exist energy-critical point. Then, it is impossible to have a single dam height that can make the battery energy-critical at any time  $t > \tau$ .

Case  $\tau_1^{opt} < \tau$ , illustrated in Fig. 13(b). We must have  $w_1^{opt} > w$  because the dam height  $w$  does not make the battery energy-critical at any time  $t < \tau$ , we have to raise the dam to make the energy-critical at  $\tau_1^{opt}$ . We claim that in the optimal dam heights, there is at least one dam height  $w_i^{opt}$  in (or partially in) duration  $[\tau_1^{opt}, \tau]$ , such that  $w_i^{opt} < w$ . Otherwise, optimal dam heights in  $[0, \tau)$  are all greater than  $w$ , contradicting the fact that  $w$  depletes battery at  $\tau$ . This is a contradiction to Lemma 5.

Therefore, the first optimal changing point  $\tau_1^{opt} = \tau$ . In this way, the size of the problem becomes smaller. By using the proof again, we can show that the algorithm can compute the optimal HTT schedule for the offline problem.

Next, we prove that the algorithm has a time complexity of  $O(T^2 \log(\frac{\rho_{max}}{\Delta})/\Delta t)$ . From Theorem 4 we could know that the algorithm `dam_raising_shotg` has a time complexity of  $O(T \cdot \log(\frac{\rho_{max}}{\Delta}))$ . In every **while** loop, we at least let  $\tau_0$  increase  $\Delta t$ . Because the worst situation is that we couldn't raise the dam, therefore,  $\tau = \tau_0$ . In the worst situation we assign  $\tau + \Delta t$  to  $\tau_0$ , that is, let  $\tau_0$  increase  $\Delta t$ . Therefore, in every **while** loop, we at least let  $\tau_0$  increase  $\Delta t$ . As a result, the **while** loop will at most run  $T/\Delta t$  times. In every **while** loop, we will run `dam_raising_shotg` once and its time complexity is  $O(T \cdot \log(\frac{\rho_{max}}{\Delta}))$ . We also run `find_emptyP` once and its time complexity is  $O(T)$ . Therefore, the time complexity of each **while** loop is  $\max(O(T \cdot \log(\frac{\rho_{max}}{\Delta})), O(T)) = O(T \cdot \log(\frac{\rho_{max}}{\Delta}))$ . Note that we just proved that the **while** loop will at most run  $T/\Delta t$  times. Therefore, the algorithm has a time complexity of  $O(T/\Delta t \cdot T \cdot \log(\frac{\rho_{max}}{\Delta})) = O(T^2 \log(\frac{\rho_{max}}{\Delta})/\Delta t)$ .

## REFERENCES

- [1] J. Li, Y. Meng, L. Zhang, G. Chen, Y. Tian, H. Zhu, and X. S. Shen, "MagFingerprint: A Magnetic Based Device Fingerprinting in Wireless Charging," in Proc. IEEE INFOCOM 2023, pp. 1-10, IEEE, 2023.
- [2] W. Zhou, H. Zhou, X. Cui, X. Wang, X. Wang, and Z. Liu, "Roland: Robust in-band parallel communication for magnetic MIMO wireless power transfer system," in Proc. IEEE INFOCOM 2023, pp. 1-10, IEEE, 2023.
- [3] M. Ren, D. Wu, J. Xue, W. Xu, J. Peng, and T. Liu, "Utilizing the Neglected Back Lobe for Mobile Charging," in Proc. IEEE INFOCOM 2023, pp. 1-10, IEEE, 2023.
- [4] Y. Ma, D. Wu, M. Ren, J. Peng, J. Yang, and T. Liu, "Concurrent Charging with Wave Interference," in Proc. IEEE INFOCOM 2023, pp. 1-10, IEEE, 2023.
- [5] P. Zhou, C. Wang, and Y. Yang, "Design and Optimization of Electric Autonomous Vehicles with Renewable Energy Source for Smart Cities," in Proc. IEEE INFOCOM 2021, July 2020, pp. 1399-1408.
- [6] R. Guida, E. Demirors, N. Dave, and T. Melodia, "Underwater Ultrasonic Wireless Power Transfer: A Battery-less Platform for the Internet of Underwater Things," IEEE Trans. Mobile Computing, to appear. Early Access, Oct. 2020.

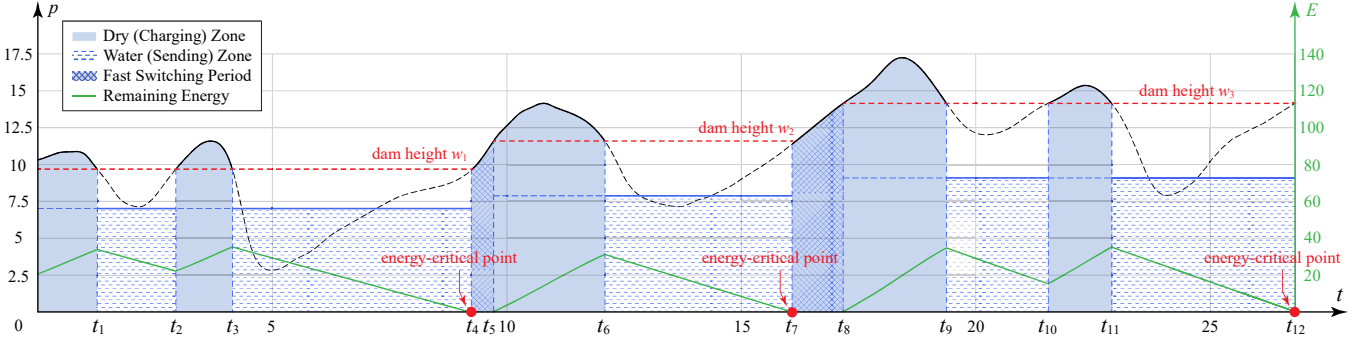


Fig. 14. An example of the optimal solution for the general harvesting power  $p(t)$ .

- [7] V. Liu, A. Parks, V. Talla, S. Gollakota, D. Wetherall, and J. Smith, "Ambient backscatter: wireless communication out of thin air," in *Proc. ACM SIGCOMM 2013*, Aug. 2013, pp. 39-50.
- [8] S. Mohanti, E. Bozkaya, M. Y. Naderi, B. Canberk, G. Secinti, and K. R. Chowdhury, "WiFED Mobile: WiFi Friendly Energy Delivery With Mobile Distributed Beamforming," *IEEE/ACM Trans. Netw.*, vol. 29, no. 3, pp. 1362-1375, Jun. 2021.
- [9] V. Iyer, V. Talla, B. Kellogg, S. Gollakota, and J. R. Smith, "Inter-technology backscatter: Towards internet connectivity for implanted devices," in *Proc. ACM SIGCOMM 2016*, Aug. 2016, pp. 1-14.
- [10] Powercast, "About Powercast," <https://www.powercastco.com>, accessed Nov. 29, 2023.
- [11] WISP, "Wireless Identification and Sensing Platform (WISP)," <https://sites.google.com/uw.edu/wisp-wiki/home> accessed Nov. 29, 2023.
- [12] S. Li, S. He, K. Hu, L. Fu, S. Chen, and J. Chen, "Operation State Scheduling towards Optimal Network Utility in RF-Powered Internet of Things," *IEEE Trans. Mobile Computing*, to appear. Early Access, May 2020.
- [13] K.-G. Nguyen, Q.-D. Vu, L.-N. Tran, and M. Juntti, "Energy Efficiency Fairness for Multi-Pair Wireless-Powered Relaying Systems," *IEEE J. Sel. Areas Commu.*, vol. 37, no. 2, pp. 357-373, Feb. 2019.
- [14] A. H. Sakr, and E. Hossain, "Analysis of K-Tier uplink cellular networks with ambient RF energy harvesting," *IEEE J. Sel. Areas Commu.*, vol. 33, no. 10, pp. 2226-2238, Oct. 2015.
- [15] T. A. Zewde, and M. C. Gursoy, "Optimal resource allocation for energy-harvesting communication networks under statistical QoS constraints," *IEEE J. Sel. Areas Commu.*, vol. 37, no. 2, pp. 313-326, Feb. 2019.
- [16] F. Shan, J. Luo, W. Wu and X. Shen, "Optimal wireless power transfer scheduling for delay minimization," in *Proc. IEEE INFOCOM 2016*, April 2016, pp. 1-9.
- [17] F. Shan, J. Luo, W. Wu, and X. Shen, "Delay Minimization for Data Transmission in Wireless Power Transfer Systems," *IEEE J. Sel. Areas Commu.*, vol. 37, no. 2, pp. 298-312, 2019.
- [18] M. A. Qureshi, and C. Tekin, "Online Bayesian Learning for Rate Selection in Millimeter Wave Cognitive Radio Networks," in *Proc. IEEE INFOCOM 2020*, July 2020, pp. 1449-1458.
- [19] H. Ju, and R. Zhang, "Throughput maximization in wireless powered communication networks," *IEEE Trans. Wireless Commu.*, vol. 13, no. 1, pp. 418-428, Jan. 2014.
- [20] F. Zhao, L. Wei, and H. Chen, "Optimal time allocation for wireless information and power transfer in wireless powered communication systems," *IEEE Trans. Vehicular Tech.*, vol. 65, no. 3, pp. 1830-1835, March 2016.
- [21] X. Song, and K.-W. Chin, "Maximizing Packets Collection in Wireless Powered IoT Networks with Charge-or-Data Time Slots," *IEEE Trans. on Cognitive Commu. and Netw.*, vol. 9, no. 4, pp. 1067-1079, Aug. 2023.
- [22] C. Jin, F. Hu, Z. Ling, Z. Mao, Z. Chang, and C. Li, "Transmission optimization and resource allocation for wireless powered dense vehicle area network with energy recycling," *IEEE Trans. Vehicular Tech.*, vol. 71, no. 11, pp. 12291-12303, Nov. 2022.
- [23] H. Kim, T. Cho, J. Lee, W. Shin, and H. V. Poor, "Optimized Shallow Neural Networks for Sum-Rate Maximization in Energy Harvesting Downlink Multiuser NOMA Systems," *IEEE J. Sel. Areas Commu.*, vol. 39, no. 4, pp. 982-997, April 2021.
- [24] M. Zhang, J. Huang, and R. Zhang, "Wireless power transfer with information asymmetry: A public goods perspective," *IEEE Trans. Mobile Computing*, vol. 20, no. 1, pp. 276-291, Jan. 2021.
- [25] R. M. Corless, G. H. Gonnet, D. E. G. Hare, D. J. Jeffrey and D. E. Knuth, "On the Lambert W Function," *Advances in Computational Mathematics*, vol 5, pp. 329-359, 1996.
- [26] J. Yang and S. Ulukus, "Optimal packet scheduling in an energy harvesting communication system," *IEEE Trans. Commun.*, vol. 60, no. 1, pp. 220-230, Jan. 2012.
- [27] Wang, B., Yang, X., Wang, G., Yu, G., Zang, W., and Yu, M. "Energy efficient approximate self-adaptive data collection in wireless sensor networks," *Frontiers of Computer Science* 10 (2016): 936-950.
- [28] B. Clerckx, J. Kim, K. W. Choi, and D. I. Kim, "Foundations of Wireless Information and Power Transfer: Theory, Prototypes, and Experiments," *Proc. IEEE*, vol. 110, no. 1, pp. 8-30, 2022.
- [29] S. Shen, J. Kim, and C. Song, "Wireless Power Transfer With Distributed Antennas: System Design, Prototype, and Experiments," *IEEE Trans. Ind. Electron.*, vol. 68, no. 11, pp. 10868-10878, Nov. 2021.
- [30] O. L. Alcaraz Lopez, O. M. Rosabal, D. E. Ruiz-Guirola, P. Raghuanthi, K. Mikhaylov, L. Loven, and S. Lyer, "Energy-Sustainable IoT Connectivity: Vision, Technological Enablers, Challenges, and Future Directions," *IEEE Open J. Commun. Soc.*, vol. 4, pp. 2609-2666, 2023.
- [31] O. L. Alcaraz Lopez, E. M. G. Fernandez, R. D. Souza, and H. Alves, "Wireless Powered Communications With Finite Battery and Finite Blocklength," *IEEE Trans. Commun.*, vol. 66, no. 4, pp. 1803-1816, Apr. 2018.
- [32] R. Valentini, M. Levorato, and F. Santucci, "Optimal Aging-Aware Channel Access and Power Allocation for Battery-Powered Devices With Radio Frequency Energy Harvesting," *IEEE Trans. Commun.*, vol. 66, no. 11, pp. 5773-5787, Nov. 2018.
- [33] L. Huang, R. Nan, K. Chi, Q. Hua, K. Yu, N. Kumar, and M. Guizani, "Throughput Guarantees for Multi-Cell Wireless Powered Communication Networks With Non-Orthogonal Multiple Access," *IEEE Trans. Veh. Technol.*, vol. 71, no. 11, pp. 12104-12116, Nov. 2022.
- [34] H.-H. Choi, M. Levorato, and H. V. Poor, "Harvest-Or-Access: Slotted ALOHA for Wireless Powered Communication Networks," *IEEE Trans. Veh. Technol.*, vol. 68, no. 11, pp. 11394-11398, Nov. 2019.
- [35] G. Karadag, M. S. Iqbal, and S. Coleri, "Optimal Power Control, Scheduling, and Energy Harvesting for Wireless Networked Control Systems," *IEEE Trans. Commun.*, Vol. 69, no. 3, pp. 1789-1801, Mar. 2021.



**Feng Shan** (Member, IEEE) received the Ph.D. degree in computer science from Southeast University, Nanjing, China, in 2015. He was a visiting student with the School of Computing and Engineering, University of Missouri-Kansas City, Kansas City, MO, USA, from 2010 to 2012. He is currently an Associate Professor with the School of Computer Science and Engineering, Southeast University. His research interests include the areas of Internet of Things, wireless networks, swarm intelligence, and algorithm design and analysis.



**Junzhou Luo** (Member, IEEE) received the B.Sc. degree in applied mathematics and the M.S. and Ph.D. degrees in computer network, all from Southeast University, China, in 1982, 1992, and 2000, respectively. He is a full professor in the School of Computer Science and Engineering, Southeast University. He is a member of the IEEE Computer Society and co-chair of IEEE SMC Technical Committee on Computer Supported Cooperative Work in Design, and he is a member of the ACM and Co-Chair of the ACM China Awards Committee. His

research interests are network architecture, network security, cloud computing, wireless network, and internet of things.



**Qiao Jin** is currently pursuing his B.Sc degree in the School of Computer Science and Engineering, Southeast University, Nanjing, China. His research interests include algorithm design and high performance computing.



**Liwen Cao** is currently pursuing his B.Sc degree in the School of Computer Science and Engineering, Southeast University, Nanjing, China. His research interests include computer vision and optimization algorithms.



**Weiwei Wu (M'14)** received his BSc degree in South China University of Technology (SCUT, Computer Science) in 2006 and the PhD degree from City University of Hong Kong (CityU, Computer Science) and University of Science and Technology of China (USTC) in 2011, and went to Nanyang Technological University (NTU, Mathematical Division, Singapore) for post-doctorial research in 2012. He is currently a Professor in Southeast University, School of Computer Science and Engineering, P.R. China. His research interests include optimizations

and algorithm analysis, crowdsourcing, reinforcement learning, game theory, wireless communications and network economics.



**Zhen Ling** (Member, IEEE) received the B.S. degree from Nanjing Institute of Technology, Nanjing, China, in 2005, and the Ph.D. degree in computer science from Southeast University, Nanjing, in 2014. He is a Professor with the School of Computer Science and Engineering, Southeast University. His research interests include network security, privacy, and Internet of Things. Prof. Ling won the ACM China Doctoral Dissertation Award in 2014 and the China Computer Federation Doctoral Dissertation Award in 2015.



**Fang Dong** is currently a full professor in School of Computer Science and Engineering, Southeast University, China. He received his Ph.D. degree in Computer Science from Southeast University in 2011. His current research interests include edge intelligence, cloud computing and Industrial Internet. He is a member of both IEEE and ACM, he also served as the co-chair of ACM Nanjing Chapter.